THE UNIVERSITY OF MICHIGAN

7260-2-Q

Technical Report ECOM-01263-2 30 November 1965

Broadband Antenna Techniques Study

Second Quarterly Report
1 July through 30 September 1965

Report No. 2

Contract No. DA-28-043 AMC-01263(E)
DA Project No. 5A0-21101-A902-01-08

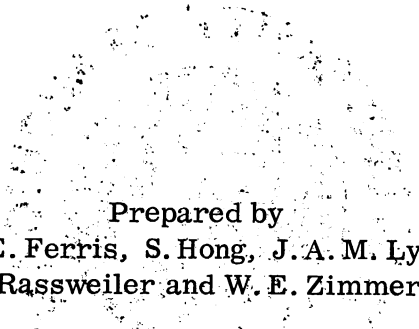

Prepared by
J. E. Ferris, S. Hong, J. A. M. Lyon,
G. G. Rassweiler and W. E. Zimmerman

The University of Michigan
Department of Electrical Engineering
Radiation Laboratory
Ann Arbor, Michigan 48108

For

United States Army Electronics Command, Fort Monmouth, N. J.

ABSTRACT

Work on the design, fabrication and testing of three broadband antennas is described. The antenna types are, 1) high-gain constant beamwidth, 2) omnidirectional and 3) loaded conical helix.

During this reporting period the optimum F/D ratio for the reflector of the high-gain constant beamwidth antenna has been determined. A decision has also been made to have the reflector surface fabricated from fiberglass, and, therefore, a plaster mold has been constructed. In the proposal, several techniques were suggested by which the constant beamwidth characteristics of the antenna could be achieved. During this reporting period the feasibility of using a wire grid structure as a reflecting surface has been considered and is reported.

Four antenna types have been considered to meet the omnidirectional antenna requirements. The antenna types considered were biconical, crossed plate, spiraled trapezoid and a random length array. A thorough discussion of the biconical antenna is included, which demonstrates both its advantages and disadvantages. Also a discussion of dipole vs. monopole configurations is included to aid in the understanding of the problem associated with broadband omnidirectional antennas.

A theoretical solution for the size reduction of a helix antenna loaded with a full core of magneto-dielectric material is discussed. The reduction formula indicates the permittivity to be more important than the permeability of the loading material. Experimental far-field patterns of the loaded helix antenna are shown which partially support the analysis.

FOREWORD

This report was prepared by the University of Michigan Radiation Laboratory of the Department of Electrical Engineering under United States Army Electronics Command Contract No. DA 28-043 AMC-01263(E). The contract was initiated under United States Army Project No. 5A0-21101-A902-01-08, "Broadband Antenna Techniques Study". The work was administered under the direction of the Electronics Warfare Division, Advanced Techniques Branch at Fort Monmouth, New Jersey. Mr. Anthony DiGiacomo is the Project Manager and Mr. George Haber is the Contract Monitor.

The material reported herein represents the results of the preliminary investigation into techniques applicable to the design and development of broadband antennas.

The authors wish to acknowledge the contributions of Professor C. T. Tai and E. Andrade for their work on the omnidirectional antenna.

TABLE OF CONTENTS

		Page
	ABSTRACT	iii
	FOREWORD	iv
	LIST OF ILLUSTRATIONS	vi
I	INTRODUCTION	1
II	BROADBAND CONSTANT BEAMWIDTH HIGH-GAIN ANTENNA	2
	2.1 Theoretical Study	2
	2.2 Constant Beamwidth Structure	9
	2.3 Experimental Study	11
	2.4 Casting Materials	11
III	OMNIDIRECTIONAL BROADBAND ANTENNA	16
	3.1 Dipole vs. Monopole	16
	3.1.1 Dipoles	16
	3.1.2 Monopoles	18
	3.2 Broadband Antenna Elements	19
	3.2.1 Conical Antenna	19
	3.2.2 Crossed Plate Antenna	22
	3.2.3 Spiraled Trapezoid	23
	3.2.4 Random Length Array	23
IV	LOADED CONICAL HELIX ANTENNA	27
	4.1 Propagation Constant	27
	4.2 Size Reduction for Bifilar Helices	30
	4.3 Discussion	33
	4.4 Experimental Results	34
	4.5 Discussion of Possible Prototype	34
V	REFERENCES	42
	DISTRIBUTION	44
	DD 1473	47

LIST OF ILLUSTRATIONS

		Page
1	Coordinate System for the Parabolic Reflector	5
2	Antenna Feed Position	5
3	Attenuation in the Pillbox as a Function of θ	6
4	Reflected Power vs. Frequency for Evenly Spaced Wire Grid of Radius r and Spacing a; $0.03 \leq a/\lambda \leq 0.30$	10
5	Reflected Power vs. Frequency for Evenly Spaced Wire Grid of Radius r and Spacing a; $0.05 \leq a/\lambda \leq 0.50$	10
6	Front View of Reflector Mold and Scraper	14
7	Back View of Mold Showing Rib and Screen Framework	15
8	Center Fed Dipole	17
9	Axially Fed Dipole	17
10	Biconical Antenna	21
11	Ground Plane Sources	21
12	Spiraled Trapezoid Antenna	24
13	Random Length Array	25
14	The Sheath Helix Loaded with Magneto-Dielectric Material	28
15	Brillouin Diagram for a Material Loaded Bifilar Helix	31
16	Helix with Dielectric Loading	37
17	Helix with Thick Layer Ferrite Loading	38
18	Helix with Thick Layer Ferrite Loading	39
19	Helix with Thin Layer Ferrite Loading	40
20	Proposed Prototype for Loaded Conical Log-Spiral Antenna	41

I

INTRODUCTION

This contract is divided into three tasks; 1) broadband constant beamwidth high-gain antenna, 2) omnidirectional broadband antenna and 3) broadband loaded conical helix.

Under Task 1, a high-gain antenna is to be developed that covers the frequency range 1 - 10 GHz. The beamwidth is to vary less than 2:1 such that a relatively constant gain of 20 db above an isotropic source is achieved with a VSWR less than 3:1 with respect to a 50 ohm load. The investigation is to include a theoretical and experimental study of broadband, constant beamwidth, high-gain antennas. Electronic switching, electromechanical or mechanical motion to effect the constant beamwidth characteristics of the antenna are not to be considered. As a result, the constant beamwidth characteristics must be achieved employing antenna beam shaping techniques.

Under Task 2, a broadband omnidirectional antenna of the monopole or dipole configuration is to be developed which will be operational over the frequency range of 100 MHz to 1 GHz having a VSWR of less than 3:1 with respect to a 50 ohm load. It is desired that the configuration be as thin as possible and its overall length comparable to that of a half-wave dipole at the low end of the frequency band (100 MHz). The maximum diameter of the configuration is to be less than 20 inches.

The objective of Task 3 is to design a circularly polarized antenna covering the frequencies of 50 MHz to 1.1 GHz, with a 2:1 reduction in size, and a maximum weight of 20 lbs. The antenna is to be a loaded conical helix. Various loading techniques are to be investigated including ferrites and dielectrics. The conical sections of the antenna may be truncated with the possibility that one may be set within the other. Cross-over networks which cause different sections to operate at different frequencies may be required.

Preliminary work on these tasks was reported in the first quarterly report (Ferris et al, 1965).

II

BROADBAND CONSTANT BEAMWIDTH HIGH-GAIN ANTENNA

During this portion of the study, a broadband high-gain antenna is to be designed and developed. The gain of the antenna is to be approximately 20 db and must be constant over a bandwidth of 10:1 (1 - 10 GHz) with a beamwidth variation of less than 2:1 across the frequency band. Since a beamwidth variation of less than 2:1 is allowed, it implies that the gain of the antenna may vary approximately 6 db and still be within specifications. The study is to include both theoretical and experimental work. The theoretical work is to provide information needed in the design and fabrication of antennas required to meet the specifications. The experimental work is required to verify the theoretical analysis and to demonstrate that the design criterias are adequate for developing a broadband constant beamwidth high-gain antenna.

2.1 Theoretical Study

Several techniques have been suggested that may be employed to achieve a broadband constant beamwidth high-gain antenna. Three techniques are the use of a reflector with 1) absorber, 2) holes and 3) a radial wire grid structure. Each of these techniques has been considered further, and to obtain a better understanding of a broadband reflecting surface, the use of a uniformly spaced wire grid structure is now being studied. The justification for using this type of structure, is the ease with which a theoretical analysis may be made. It is anticipated that from this theoretical analysis and an experimental study, a better understanding of broadband high-gain antenna techniques will be obtained.

As evidence by the present study, a desirable feature of a broadband high-gain antenna is the feasibility of having a relatively constant beamwidth over a wide frequency range. The present study is concerned with limiting the beamwidth variation of the parabolic antenna to less than 2:1 for a frequency range of 10:1. The use of an equally spaced wire grid reflecting surface is presently being investigated to effect such a design. Early work in this program was confined to a pillbox, therefore, the following theoretical analysis will be concerned with a pillbox structure, which may be expanded to a two-dimensional parabolic reflector later.

The equation of the parabolic curve used for the back wall may be expressed in polar coordinates as:

$$r = \frac{2p}{1 + \cos\theta} \qquad (1)$$

where r is the distance from the origin to the curve, and θ is the angle from the y axis to r. Figures 1 and 2 depict the curve, coordinate system, and the position of the feed in the antenna. It will be noted that the power from the feed will experience an attenuation proportional to $1/r$ as it propagates toward the reflecting surface, (since the field radiates with a cylindrical wavefront in the pillbox).

To determine the reflector distribution, it is necessary to determine the space attenuation effects within the pillbox. Since the point of minimum loss occurs at $\theta = 0^{o}$, which corresponds to $r = p$, the loss at $r = r_n$ is expressed as:

$$10 \log \frac{r_n}{p} = 10 \log \frac{2}{1 + \cos \theta} \tag{2}$$

This result appears graphically in Fig. 3 for $\theta \leq 120^{o}$. From Fig. 1 and 2, it can be seen that

$$\theta = (\phi + \beta) \tag{3}$$

β has been chosen to be $62\ 1/2^{o}$ to optimize the pillbox aperture distribution. The space attenuation effects may now be added directly to the antenna feed pattern to obtain the illumination over the reflector.

The effective aperture of the pillbox as a function of θ may now be found. Recall from equation (1) that $r = 2p/(1 + \cos \theta)$. By inspection of Fig. 1 and 2,

$$x = r \sin \theta = \frac{2p \sin \theta}{1 + \cos \theta} \tag{4}$$

In this case, $p = 13$ inches so that

$$x_n = \frac{26 \sin (\phi + 62\ 1/2^{o})}{1 + \cos (\phi_n + 62\ 1/2^{o})} \tag{5}$$

Let ϕ_1 be the angle at which the first -10 db ray of the primary feed intercepts the reflector and let ϕ_2 be the second -10 db ray that intercepts the reflector. The effective aperture size is then given by:

$$L = x_2 - x_1 \tag{6}$$

Finally, the 3 db beamwidths of the pillbox may be approximated by:

$$\psi = \frac{K\,57^{o}\lambda}{L} \tag{7}$$

where K is a function of the aperture distribution (e.g. K = 1.2 for a cosine distribution), and λ is the wavelength. The results are tabulated in section 1 of Table I. Notice that the results are in good agreement with the experimental data, differing only by a factor of 0.64. In each case, the beamwidth variation is very nearly 3:1 over a 10:1 frequency band.

In the above discussion, it was assumed that the pattern of the primary feed was available, and the design was centered about this information. An alternate approach is to assume the pattern of the primary feed is not available and must be determined analytically such that the following discussion is applicable.

For this case, the pillbox feeds will be limited to H-plane sectorial horns such that the phase variation across the aperture is $\leq \lambda/16$; the amplitude taper may be expressed as A cos ϕ, where ϕ is the angle from a normal to the plane of the aperture as shown in Fig. 2. Allowing ℓ to be the length of the primary feed aperture, the far field amplitude distribution is given by:

$$E_F = \frac{\pi \ell}{2} \frac{\cos u}{\left[\frac{\pi}{2}\right]^2 - u^2} \tag{8}$$

where

$$u = \frac{\pi \ell}{\lambda} \sin \phi$$

Neglecting multiplicative constants, $E_F = A \dfrac{\cos u}{\left[\frac{\pi}{2}\right]^2 - u^2}$ (9)

Figure 2 describes the orientation of the sectorial feed in the pillbox. If β is the angle between the y axis and the line normal to the feed aperture, the variable ϕ in equations (8) and (9) may be expressed in terms of the new variable θ as:

$$\phi = (\theta - \beta) \tag{10}$$

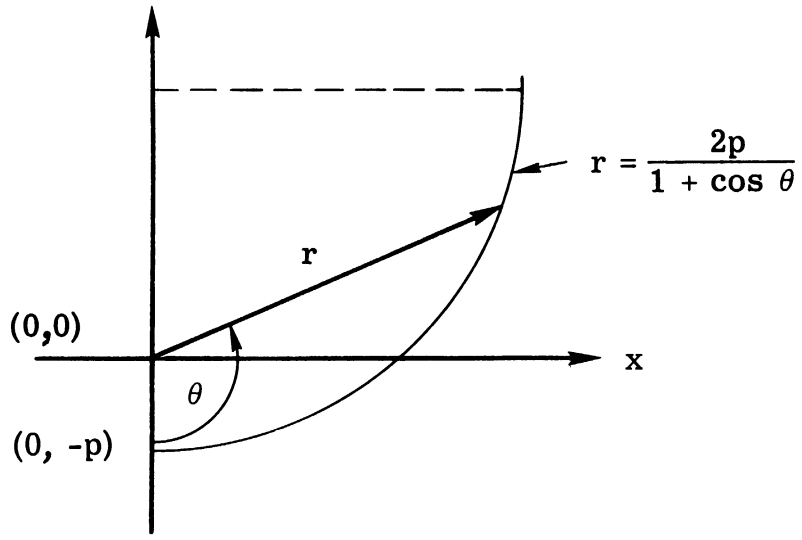

FIG. 1: PARABOLIC REFLECTOR COORDINATE SYSTEM

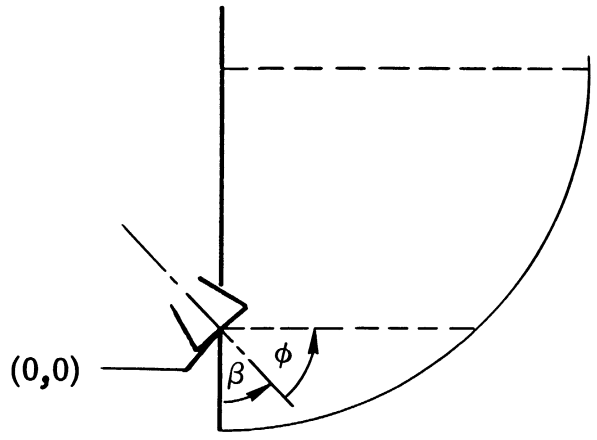

FIG. 2: ANTENNA FEED POSITION

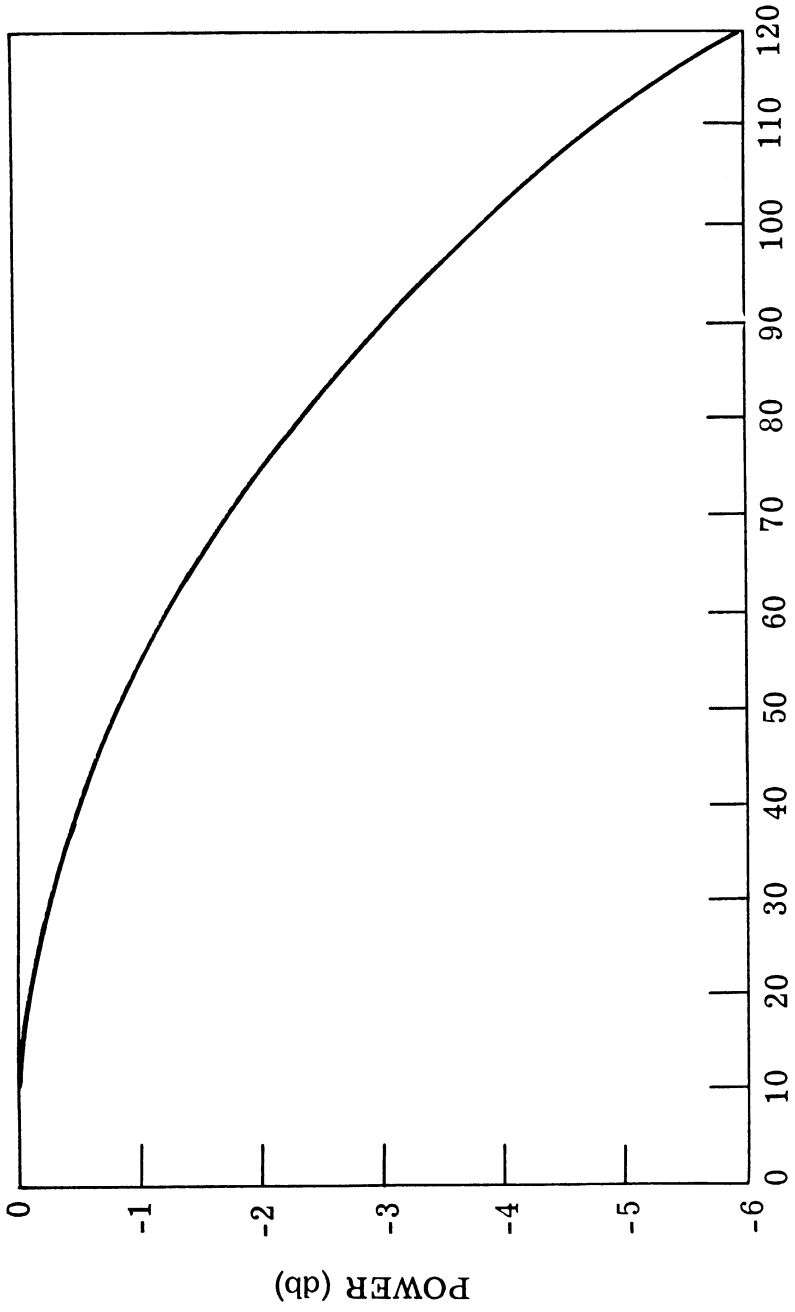

FIG. 3: ATTENUATION IN THE PILLBOX AS A FUNCTION OF θ

TABLE I: Feed And Antenna Beamwidths

Frequency (GHz)	Feed 10 db BW (Degrees)	Illum. 10 db BW (Degrees)	Eff. Ap. (Inches)	3 db Ant. BW (Degrees)	Exper. BW (Degrees)
		Section I Solid Reflector			
1	102	100	31	26	16
2.5	86	82.5	22.5	14	9
5.3	45	44	13	12	7
10.0	26	29	9	9	5.5
		Section II Wire Grid; $0.03 \leq a/\lambda \leq 0.30$, $\frac{a}{r} = 50$			
1	102	100	31	26	--
2.5	86	82.5	22.5	14	--
5.3	45	39	11	14	--
10.0	26	17.5	5	16	--
		Section III Wire Grid; $0.05 \leq a/\lambda \leq 0.50$, $\frac{a}{r} = 50$			
1	102	100	31	26	--
2.5	86	78	20	16	--
5.3	45	26.5	8	19	--
10.0	26	20	5	16	--

thus $$E_F = A \frac{\cos u}{\left[\frac{\pi}{2}\right]^2 - u^2} \quad \text{where } u = \frac{\pi \ell}{\lambda} \sin(\theta - \beta) \tag{11}$$

This is an expression of the magnitude of the electric vector in the Fraunhofer field of the sectorial feed, expressed in the coordinate system established within the pillbox.

The power distribution along the parabolic reflecting surface will vary as $1/r$, (recall that the antenna is essentially only two-dimensional, restricting the wavefront in the z direction). Since $r = 2p/(1 + \cos\theta)$, the magnitude of the electric field at the reflector surface E_R may be given as:

$$E_R = A\left[\frac{1 + \cos\theta}{2p}\right]^{1/2} \frac{\cos u}{\left[\frac{\pi}{2}\right]^2 - u^2} \tag{12}$$

Since the rays reflected from the back wall of the pillbox will be collimated after reflection, no attenuation of the wavefront will occur. The amplitude distribution at the aperture of the pillbox as a function of x will then be the same as the amplitude distribution at the back wall as a function of the same variable. The phase distribution across the pillbox aperture will be constant because of the geometrical properties of the parabolic surface of the back wall. Using the relations:

$$E_R(\theta) = A\left[\frac{1 + \cos\theta}{2p}\right]^{1/2} \cdot \frac{\cos u}{\left[\frac{\pi}{2}\right]^2 - u^2}, \quad u = \frac{\pi \ell}{\lambda} \sin(\theta - \beta)$$

and $$x = \frac{2p \sin\theta}{1 + \cos\theta}, \quad \text{from } x = r\sin\theta, \quad r = \frac{2p}{1 + \cos\theta} \tag{13}$$

one may express the amplitude of the electric field across the aperture as a function of x,

$$E_A(x) = f(x). \tag{14}$$

The far field pattern of the pillbox may then be expressed as:

$$E(u') = B \int_{-1}^{1} E_A(x')\, e^{ju'x'}\, dx' \qquad (15)$$

where x' is the distance x along the aperture normalized to 1, and

$$u' = \frac{\pi L}{\lambda} \sin \alpha \qquad (16)$$

L being the length of the pillbox aperture and α the angle from a normal to the plane of the aperture at the aperture center.

Thus far it has been assumed that: 1) the phase variation across the sectorial feed horn is $\leq \lambda/16$, and that the amplitude taper is a simple cosine function, 2) diffraction effects at the edges of the feed may be neglected, 3) the reflecting surface may be considered to be in the far field of the feed, 4) "spill-over", i.e. energy radiated by the feed not intercepted by the reflector may be neglected, 5) diffraction effects at the edges of the pillbox aperture may be neglected, 6) there are no stray reflections within the pillbox, and 7) the reflecting surface is smooth, i.e. perfect reflecting parabolic curve.

2.2 Constant Beamwidth Structure

To further restrict the beamwidth variations the use of a modified reflecting surface is planned. Suppose now that the solid reflector is replaced by a series of equally spaced wires which will behave as a frequency sensitive reflector. However, in order that there will be adequate reflected power at the higher frequencies, a solid section is required in the center of the wire grid structure. The portion of the power transmitted through the grid can be found from the nomograph given by Mumford (1961). Assume that the power not transmitted is reflected. Figure (4) and (5) are plots of the attenuation of the reflected power in db for two different wire spacings. This new attenuation factor may now be superimposed on the original feed patterns from which a new reflector distribution and the effective pillbox aperture dimension may be obtained. Sections II and III of Table I tabulate the results. As can be seen from the analytical results, using an equally spaced wire grid reflecting surface, beamwidth variations of 2:1 over a 10:1 frequency band may be obtained. Experimental verification of these results with various spacings is at present being undertaken.

Thus far, all efforts (experimental and analytical) have been concerned with the pillbox antenna. However, the final task is the construction of a high-gain,

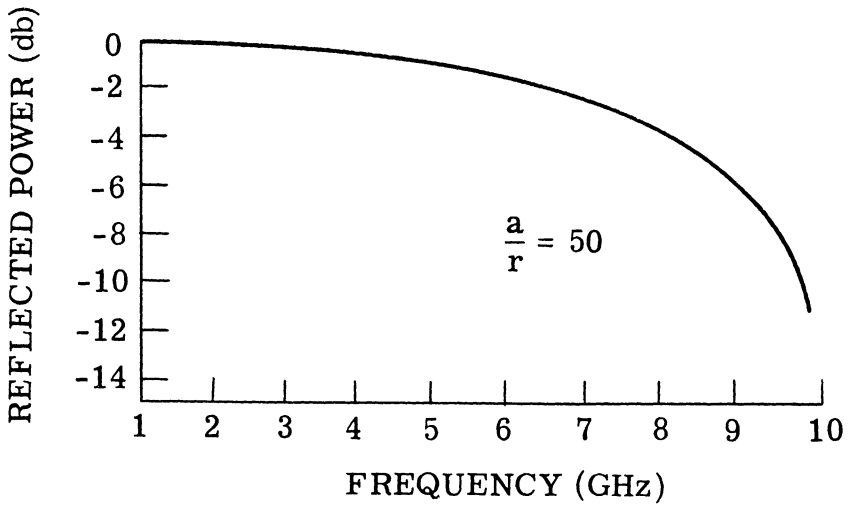

FIG. 4: REFLECTED POWER VS. FREQUENCY FOR EVENLY SPACED WIRE GRID OF RADIUS r AND SPACING a; $0.03 \leq a/\lambda \leq 0.30$.

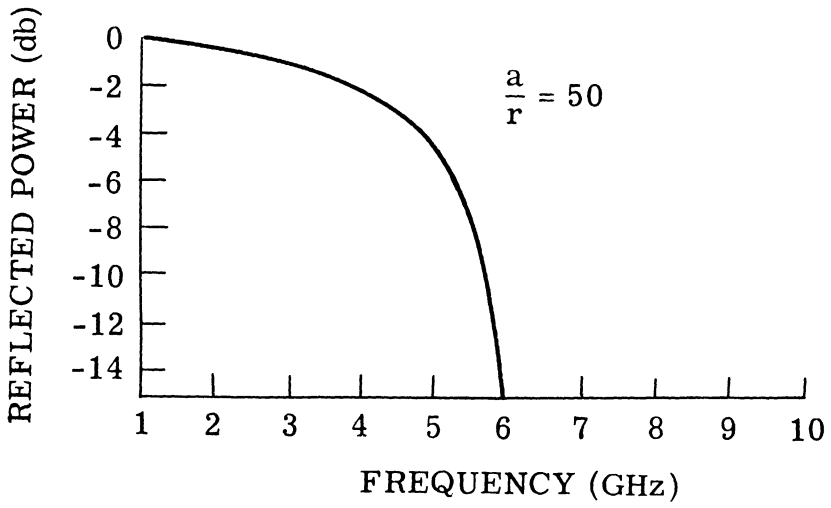

FIG. 5: REFLECTED POWER VS. FREQUENCY FOR EVENLY SPACED WIRE GRID OF RADIUS r AND SPACING a; $0.05 \leq a/\lambda \leq 0.50$.

constant beamwidth parabolic reflector. The pillbox results will be extended to this antenna in the near future.

2.3 Experimental Study

In the previous Interim Report, it was noted that the feasibility of using the broadband ridged horn had been demonstrated and it was next necessary to determine the F/D ratio of the reflector. To determine the optimum F/D ratio, a pillbox structure was employed to simulate energy radiating from the central portion of the full reflector. The principle design goal was to optimize the F/D ratio that would minimize the aperture size of the primary feed and simultaneously yield satisfactory secondary patterns. It is logical that as the F/D ratio is increased, the aperture size of the primary feed must also be increased to ensure that the beamwidths of the primary feed properly illuminates the reflector as the frequency is decreased. As a result of both an analytical and experimental investigation, the F/D ratio was chosen to be 0.25. After the F/D ratio had been selected, the construction of a full scale 2-dimensional parabolic reflector was started. The reflector will be asymmetrically fed with the broadband ridged horn. Initially, it was planned that the full scale reflector could be fabricated from a metallic alluminum sheet that had been spun to the desired contour. However, it was later concluded a less expensive and more desirable reflector could be fabricated from fiberglas.

2.4 Casting Materials

A reflector mold has been constructed and covered with dental stone. Several casting materials were considered before the choice of dental stone was made. Below is a brief discussion of the materials that were considered.

All materials considered were forms of plaster. By different processes of reduction of gypsum widely varied physical properties of the refined material are obtained. Mineral gypsum is a hydrated calcium sulfate ($CaSO_4 . 2H_2 0$) in which the water of crystallization is weakly held. The powdered material which is heated in the reduction processes may give either of two products depending upon the temperature used.

$$2CaSO_4 . 2H_2O \xrightarrow{\text{(Heat, } 350^{\circ}\text{ F)}} \underset{\text{Half-hydrate}}{2CaSO_4 . 1/2H_2O} + 3H_2O \uparrow \qquad (17)$$

or with more heat

$$CaSO_4 . 2H_2O \xrightarrow{\text{(Heat, } 400^{\circ}\text{ F)}} \underset{\text{Anhydrite}}{CaSO_4} + 2H_2O\uparrow \qquad (18)$$

The half-hydrate is generally called plaster of Paris or gypsum plaster. This is used in dentistry in two forms, model 1 (slow setting, 20 minutes) and model 2 (fast setting, 4-5 minutes). Different setting times are obtained by the temperature used in the reduction process and the size of the powdered particles.

Setting process is the recombination with water to form the hydrated calcium sulfate. Since the setting process requires water and is obtained through reaction with water, plaster is a true hydraulic cement. The solubility of the half-hydrate is about 9 grams per liter at room temperature. The dihydrate has a solubility of 2 grams per liter. When the half hydrate becomes a dihydrate a super saturated solution is formed with the dihydrate precipitating in crystalline form. This precipitation in crystalline form is the process that gives strength to the plaster.

Dental stones (both regular and improved) are a form of the anhydrite but due to rapid heating in the reduction process the $CaSO_4$ retains the crystalline structure of $CaSO_4 . 1/2H_2O$ giving a more soluble anhydrite. The reaction with water is similar, but each particle reacts somewhat slower forming crystals that are larger and stronger.

Dental stone is many times more durable than dental plaster being harder and less prone to crack. It also has the advantage of less expansion in the setting process (less than 0.5 percent) and lower heat of formation. Regular dental stone has a compressive strength of 8,000 lbs per square inch. Improved dental stone has a compressive strength of 12,000 lbs per square inch and a Rockwell C hardness of 90. No figures were available on tensile strength but it was felt that the improved dental stone would also have a higher tensile strength.

Other superior properties of improved dental stone include its low expansion (less than 0.08 percent) and a greater surface hardness. In addition it appears that the improved dental stone would have greater strength and therefore less likelihood of cracking when the form is moved. For these reasons, it was selected as the casting material.

Setting time of the plasters considered above may be accelerated by the use of potassium sulfate (K_2SO_4). The process is not clearly understood, but a 2 percent solution of K_2SO_4 will cause almost immediate setting.

Retarding the setting time is accomplished by using sodium tetraborate ($Na_2B_4O_7 \cdot 10H_2O$). A 2 percent solution may retard the setting up to 4 hours.

The reflector was made by using plywood forms sawed to the rough dimensions of the parabolic reflector. These sections were attached to a cylindrical sector of a 4" x 4" support at the vertex. The base of the mold was formed by attaching the plywood forms to a half inch plywood sheet. To provide support for the first layer of plaster the plywood forms were covered with ordinary window screen. A revolving scraper was constructed by using a metal blade machined to the parabolic form. This scraper was supported by a collar at the vertex and a circular track at the base (Fig. 6-7). In this way, the scraper was free to rotate about the principal axis of the parabolid with approximately 1/4" clearance over the plywood and screen. Successive layers of dental plaster were applied until the scraper would just touch the surface giving the desired contour. The resulting mold is extremely durable due to the greater tensile and compressive strength of improved dental stone, and contains a smooth surface, accurate to $\lambda/16$ at the highest frequency of interest (10GHz).

The mold is now being coated with fiberglas by a local manufacturer of fiberglas boats. The fiberglas is sprayed on the mold with a gun in a similar manner that undercoating is applied to automobiles. This process is less expensive and faster than manually applying the resin and fiberglas cloth. It is anticipated that the hard dental stone mold will be durable enough to obtain several reflectors of varying thickness if necessary. These will be used to optimize the broadband reflector surface, the grid structure, and in experimenting with holes in the reflector surface.

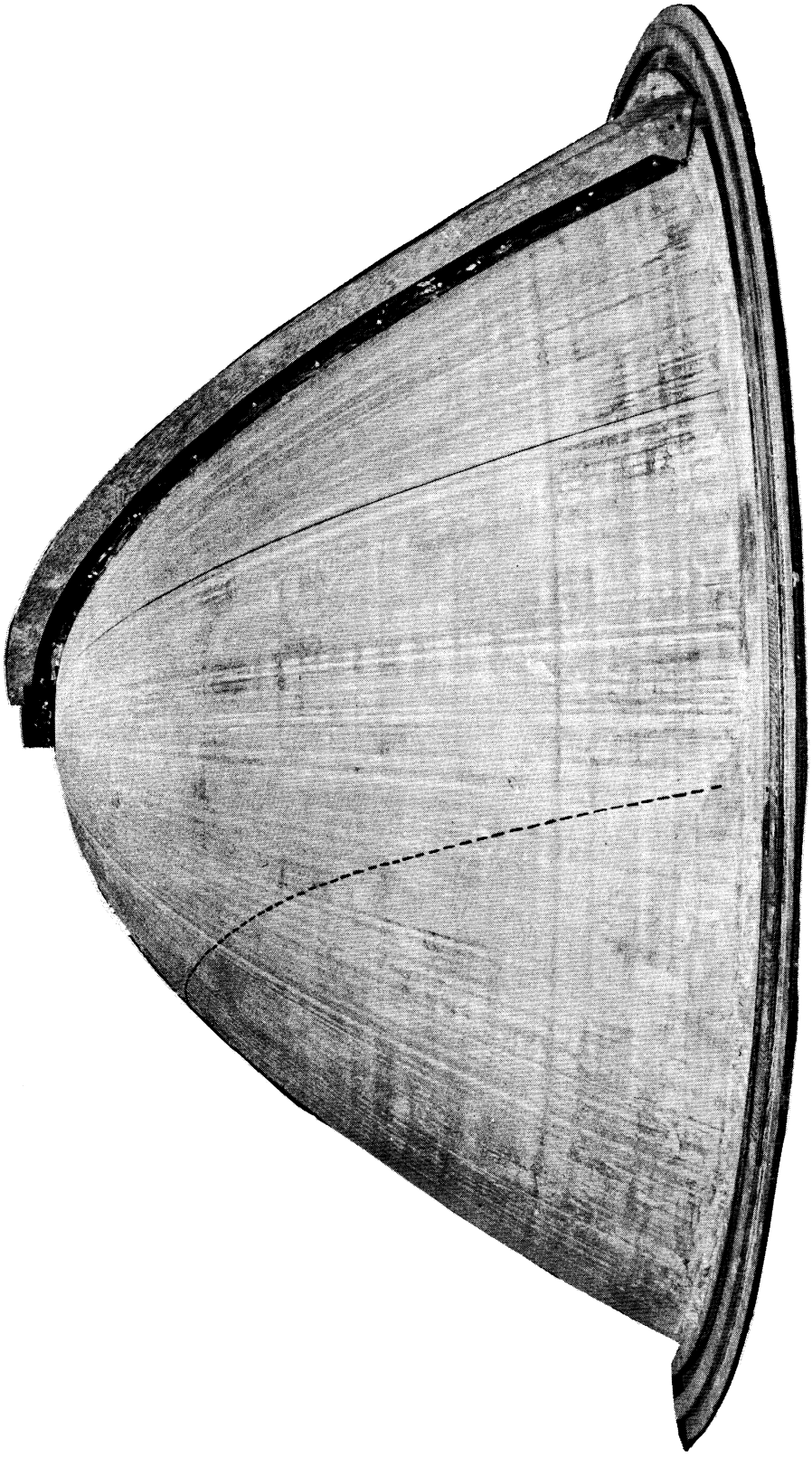

FIG. 6: FRONT VIEW OF REFLECTOR MOLD AND SCRAPER
HEIGHT = 48" - DIAMETER AT BASE = 100"

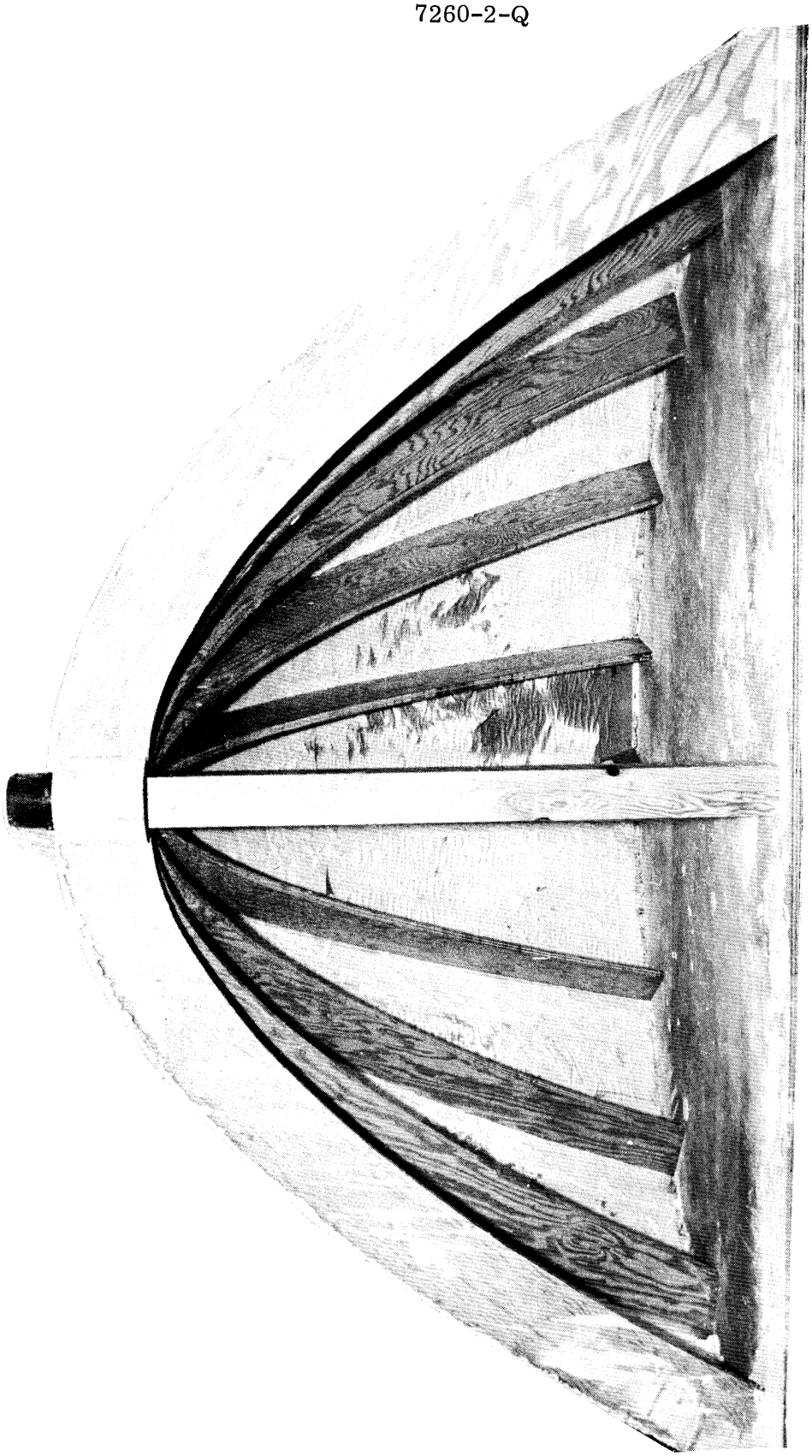

FIG. 7: BACK VIEW OF MOLD SHOWING RIB AND SCREEN FRAMEWORK

III

OMNIDIRECTIONAL BROADBAND ANTENNA

The design goals for the omnidirectional antenna are; 1) 10:1 frequency range (0.1 - 1.0 GHz), 2) 1.5 db gain with respect to an isotropic source for the above frequency range, 3) VSWR of less than 3:1 for the above frequency range, and 4) the maximum diameter of the antenna is not to exceed 20 inches. Broadband vertical radiators that have been employed in the past to achieve omnidirectional coverage are sleeve dipoles, conical dipoles and a crossed plate monopole. However, the sleeve and conical dipole typically have a 3:1 frequency range limit. Lamberty (1958) demonstrated the crossed plate to be operational over a 20:1 frequency range. Several other antenna configurations have been considered during this study which are: 1) biconical, 2) crossed plate, 3) spiraled trapezoid, and 4) array of vertical monopoles. Before discussing these, the merits of a dipole configuration versus a monopole configuration will be considered.

3.1 Dipole vs. Monopole

Dipoles have been developed which are capable of operating satisfactorily over a 3:1 frequency range, e.g. sleeve dipoles and biconicals. However, the use of these antennas for wider bandwidths, e.g. 10:1 have not been highly successful because of resonant current effects that tend to distort the radiation patterns. Before discussing dipoles, further consideration will be given to the techniques for feeding them.

3.1.1 Dipoles

There are basically two techniques for feeding the dipole configuration which are: 1) center fed, and 2) axial fed.

When employing the center fed system, it is desirable for the input line to be perpendicular to the principal plane of propagation as shown in Fig. 8. In the event the lead-in is parallel to the principal plane of the E field, currents will be induced on it and radiated to distort the radiation pattern about the axis of the dipole. A second undesirable feature of this configuration is the problem associated with mounting a vertically polarized dipole (while maintaining the lead-in horizontal) since it would be awkward and structurally weak.

An additional limitation imposed on the center fed system is the need for the antenna to be fed by a balanced line. Since, for the purposes of the present contract, the antenna is to be operational over a 10:1 frequency band, a broadband balun would be required. Ten to one baluns have been developed and reported by Duncan, et al

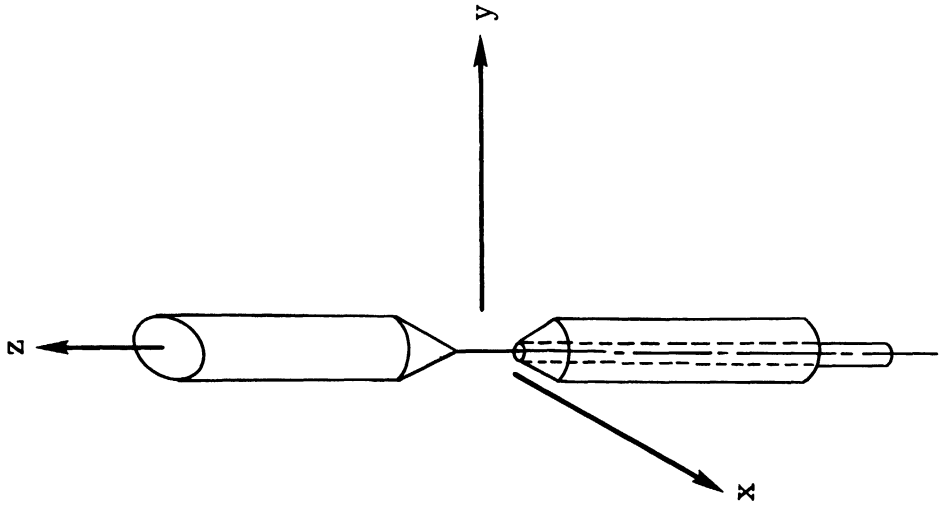

FIG. 9: AXIALLY FED DIPOLE

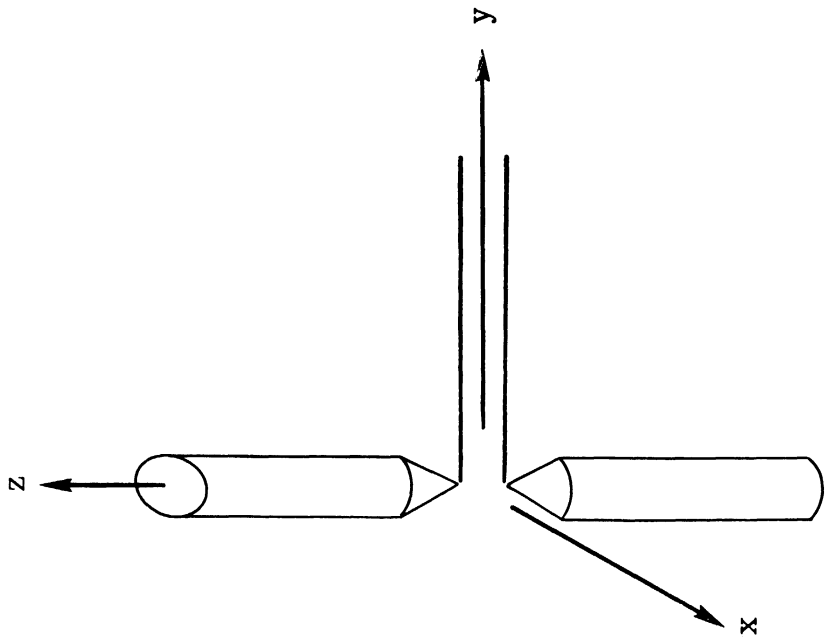

FIG. 8: CENTER FED DIPOLE

(1961) and Gans, et al (1965). Both of these baluns taper from an unbalanced system (coax or stripline) to a balanced system over an appreciable part of a wavelength such that they must be approximately $\lambda/2$ long at the lowest frequency of interest. In general, these units are not rugged and additional structural members are required.

To overcome some of the problems associated with center fed dipoles, designers often turn to the axially fed dipole (Fig. 9). This configuration eliminates the need for a balun and also simplifies the mounting problem for vertically polarized elements. Since the lead-in is fed through one of the elements of the dipole, provisions must be made to minimize currents from flowing on the lead-in. RF chokes are generally employed to minimize these currents, however, they are effective over narrow frequency bands (less than 10 percent) and therefore, are not recommended for wide band applications. To overcome the problems associated with dipoles, monopole antennas are generally recommended. However, one must be careful as to how he defines a monopole as will be shown in the next section.

3.1.2 Monopoles

A prime factor which tends to be favorable for the monopole is that it is an unbalanced antenna. The monopole in its simplest sense consists of one half of a dipole and an infinite conducting ground plane. The infinite conducting ground plane has in induced surface charge which produces a field that is identical to that which would be produced in a plane located at the center of the dipole, and normal to its axis such that the other half of the dipole is imaged in the ground plane. Since in practice it is not feasible to employ an infinite ground plane, finite ground planes are substituted. It has been shown (Lazarus, 1947) that if the finite ground plane is several wavelengths in diameter, the far field radiation patterns will be similar to those of a monopole above an infinite ground plane. As the ground plane size is reduced such that its dimensions approach the free space wavelength of the frequency being radiated, the radiation patterns become distorted in the plane containing the axis of the monopole (elevation plane). This distortion of the pattern is the result of the finite ground plane surface charges being altered. These surface charge alterations are caused by the currents reflected from the edges of the finite ground plane. Therefore, when the ground plane is large (e.g. 5λ or more) the radiation pattern is omnidirectional with its maximum along the surface of the ground plane. As the ground plane size is reduced until it becomes less than a wavelength in diameter, the pattern remains omnidirectional with its maximum intensity gradually tilting upwards to some arbitrary angle above the ground plane (Jasik, 1961). In addition to the radiation characteristics being sensitive to ground plane size, the

impedance characteristics are also sensitive as noted by (King, 1956). Therefore, the designer cannot divorce the ground plane from the antenna but must consider it a part of the antenna system.

Returning now to the requirements of the present program. Since the maximum diameter of the antenna is not to exceed 20 inches, the ground plane must not exceed 20 inches because it must be considered as a part of the antenna system. The frequency range of the antenna is to be from 0.1 - 1.0 GHz such that the free space wavelength varies from 120 - 12 inches. Because the ground plane size is to be fixed at 20 inches maximum, its electrical size will vary from 0.17λ - 1.7λ. If we consider the ground plane to be flat and therefore electrically small, the electrical characteristics of the antenna will be frequency sensitive, as noted above regardless of the electrical characteristics of the monopole element. Therefore, if one desires to have a broadband monopole antenna system, it is necessary for both the monopole and ground plane to be individually broadband elements. We must now consider the techniques applicable to achieve a broadband ground plane to satisfy the contractual requirements. One method for achieving a broadband ground plane is to employ a conical surface rather than a flat surface. A ground plane having a conical surface is analogous to using one half of a biconical antenna which is regarded as a broadband antenna configuration. However, care must be exercised in choosing the conical surface. Further discussion on the conical antenna and its broadband characteristics is therefore included in the section on broadband elements.

3.2 Broadband Antenna Elements

This section discusses several broadband element configurations. These elements may be utilized either by combining two similar elements to form a broadband dipole or by use of a single element and a suitable ground plane to form a broadband monopole. The four antenna types considered during this reporting period were the conical, crossed plate, spiraled trapezoid, and a random length array.

3.2.1 Conical Antenna

The conical antenna may be completely described in terms of angles, a general requirement of many broadband antennas. This configuration has also been shown experimentally (Brown and Woodward, Jr., 1952) to be broadbanded for a 5:1 frequency band.

To be truly broadband, an antenna must possess both acceptable VSWR and pattern characteristics over the frequency range of interest. Antennas may have acceptable impedance characteristics but unacceptable pattern characteristics.

Therefore in the development of a broadband antenna one must determine both the impedance and pattern requirements that will best solve the problem. For example, a breakup of the biconical antenna pattern into grating lobes may not be objectionable if the application requires a main beam along the horizon.

The biconical antenna basically provides a smooth transition between guided and free space waves. A criteria for a broadband antenna is for a reflectionless or near reflectionless transition. Biconical antennas of infinite length and a total included cone angle of 60^{o} (Fig. 10) or greater will set up only the TEM mode between the conical surfaces. If the cone angle is less than 60^{o} the coaxial TEM wave and biconical TEM wave will not be well matched, because of the poor transition from the coaxial line to the antenna. Practical applications of the biconical require that a finite cone length be employed. For the finite case the TEM wave is terminated at the base end of the cone where the transition to free space is accomplished by establishment of a TM wave. This TM wave has two components, an outwardly traveling wave into free space and an inwardly traveling wave toward the apex of the cones. The inward traveling TM wave is shown (Schelkunoff, 1943) to approach zero as the apexes of the cones are approached. Since the dominate field near the apexes is a TEM wave, the velocity of propagation is independent of frequency, and the characteristic impedance for a long finite biconical is essentially frequency independent. Therefore, the input impedance of the antenna is primarily controlled by the transmitted and reflected TEM waves which further determine the input VSWR. The magnitude of the reflected TEM wave is determined by the matching of the TEM field by the TM field at the biconical aperture. These two fields can be well matched only if the radius of the base of the cone is electrically large so that the $1/r^2$ and $1/r^3$ terms of the TM wave are small. Further the cone angle must be large such that the $1/\sin\theta$ component of the TEM wave is approximately equal to the $\sin\theta$ component of the TM wave. For cones having a base radius less than $\lambda/4$, the TM field in the transition region introduces a large reactive field which is significant at the apexes of the cones. This large reactive field disrupts the input impedance by introducing a large reactive component.

Consideration must now be given to pattern performance. The patterns of the biconical depends upon the ratio of the reflected to the transmitted current in the cone region, i.e. the phase and amplitude distribution of the total current. The total current includes both the TEM and TM waves. Although the TM induced currents disappear at the cone apex and do not contribute appreciably to the impedance, they are of sufficient amplitude at the base to contribute significantly to the pattern. Therefore, patterns cannot be computed from the behavior of the TEM wave alone. Although the impedance may be essentially unaffected as shown above, the pattern

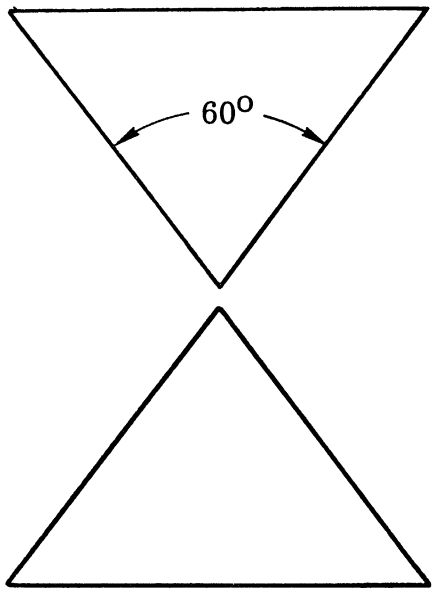

FIG. 10: BICONICAL ANTENNA

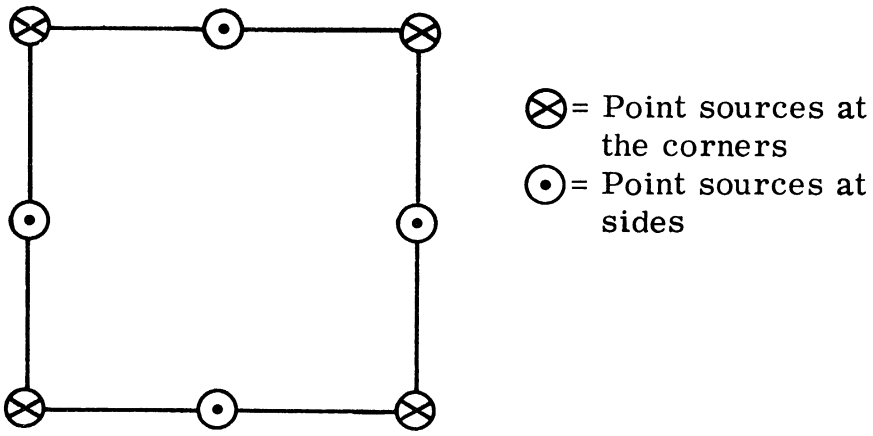

FIG. 11: GROUND PLANE SOURCE

may exhibit a lobing structure due to the discontinuity at the cone base.

For broadband applications the biconical is limited for two reasons, 1) due to impedance characteristics at the lower frequencies, and 2) due to the pattern characteristics at the higher frequencies. At the lower frequency where the antenna becomes less than $\lambda/4$ the impedance has a large mismatch due to the large reactive component as a result of the TM wave at the apex. As the frequency is increased the conical sections become several $\lambda/2$ long and a lobing of the pattern results (Brown and Woodward, 1952).

For the bandwidth and application of this project, it appears that the biconical would provide satisfactory electrical performance. However, other antennas are being investigated as to their desirability since the biconical antenna is large and cumbersome for mobile applications. Another antenna similar in size to the biconical is the crossed plate antenna discussed in the next section.

3.2.2 Crossed Plate Antenna

Elevation patterns for the crossed plate monopole appear similar to experimental patterns for a conical monopole (Brown and Woodward, Jr.). Early patterns for the azimuth plane (omni-directional) were obtained with a pair of crossed plates mounted over a square ground plane. These patterns showed poor omni-directivity. Diffraction effects at the corners and sides of the square ground plane are believed to have caused the lack of uniformity. The effect of the square ground plane may be analyzed by replacing the corners and sides of the ground plane with an array of point sources as shown in Fig. 11. The sources at the four corners produce a cloverleaf pattern which would be superimposed on the element pattern. In addition, the sources at the edges would produce a second cloverleaf pattern displaced 45° from that generated at the corners, and of a greater magnitude. This second cloverleaf pattern must also be superimposed on the element pattern. Since these two effects were observed on the data, it is felt the poor omni-directivity was caused by the square ground plane. Improved omni-directional patterns could be obtained through the use of a circular ground plane.

Data for the VSWR of the crossed plate presented in the previous quarterly exhibited several frequencies having high VSWR's. It is to be recalled that these plates were square with no tapering at the base. Preliminary data with one plate in a monopole configuration shows considerable improvement in VSWR by tapering the antenna edge at the base to form a conical transmission line. The maximum VSWR for this configuration was 2:1 across a 10:1 frequency band.

The crossed plate antenna exhibits the same physical limitation as the biconical since the elements are large and bulky. One of the main objectives during this reporting period has been to obtain a smaller physical structure, two of which will be discussed below.

3.2.3 Spiraled Trapezoid

One of the well established broadband antennas is the log periodic. However, in its normal configuration it is not suitable as an omnidirectional antenna because it produces an end fire radiation pattern. A study has been conducted to modify the log periodic such that an omnidirectional pattern could be obtained. Initially, a sheet of metal was cut into a trapezoid, i.e. a linear taper. Acceptable impedance characteristics (less than 3:1) were observed for a 10:1 frequency range. The trapezoid was then rolled into a spiral (Fig. 12). Several spiral configurations were tried before acceptable VSWR data was obtained. It is to be noted that much of this work was of the cut and try variety such that accurate physical dimensions were not obtained.

Patterns of the spiraled trapezoid were omnidirectional over a 3:1 band (in the low frequency range) and as the frequency was increased to increase the bandwidth the omnidirectional pattern degenerated to a cardioid that rotated with the frequency. Since this data did not appear promising for the present program requirements, further efforts to optimize the physical parameters of the antenna have not been tried.

3.2.4 Random Length Array

A second antenna developed from the log periodic structure is a random array of elements. Elements were cut to the proper length required for a log periodic antenna and randomly placed on a thin circular disk (Fig. 13). The VSWR of this configuration was found to be less than 3:1 over a 10:1 frequency band. Early pattern data for the antenna demonstrates that it is omnidirectional. The optimum design for the antenna has not been formalized as yet. Since the antenna appears to possess electrical characteristics that are acceptable to the present program, the study is being continued. During the continuation, efforts are being directed towards optimizing the antenna lengths and number of elements required to achieve a 10:1 frequency bandwidth. Because the antenna lengths and number have not been optimized physical dimensions have not been presented in this report. It is felt that before presenting data for the antenna, better understanding of its operation is required. Presently the experimental data is being evaluated such that future design parameters may be established.

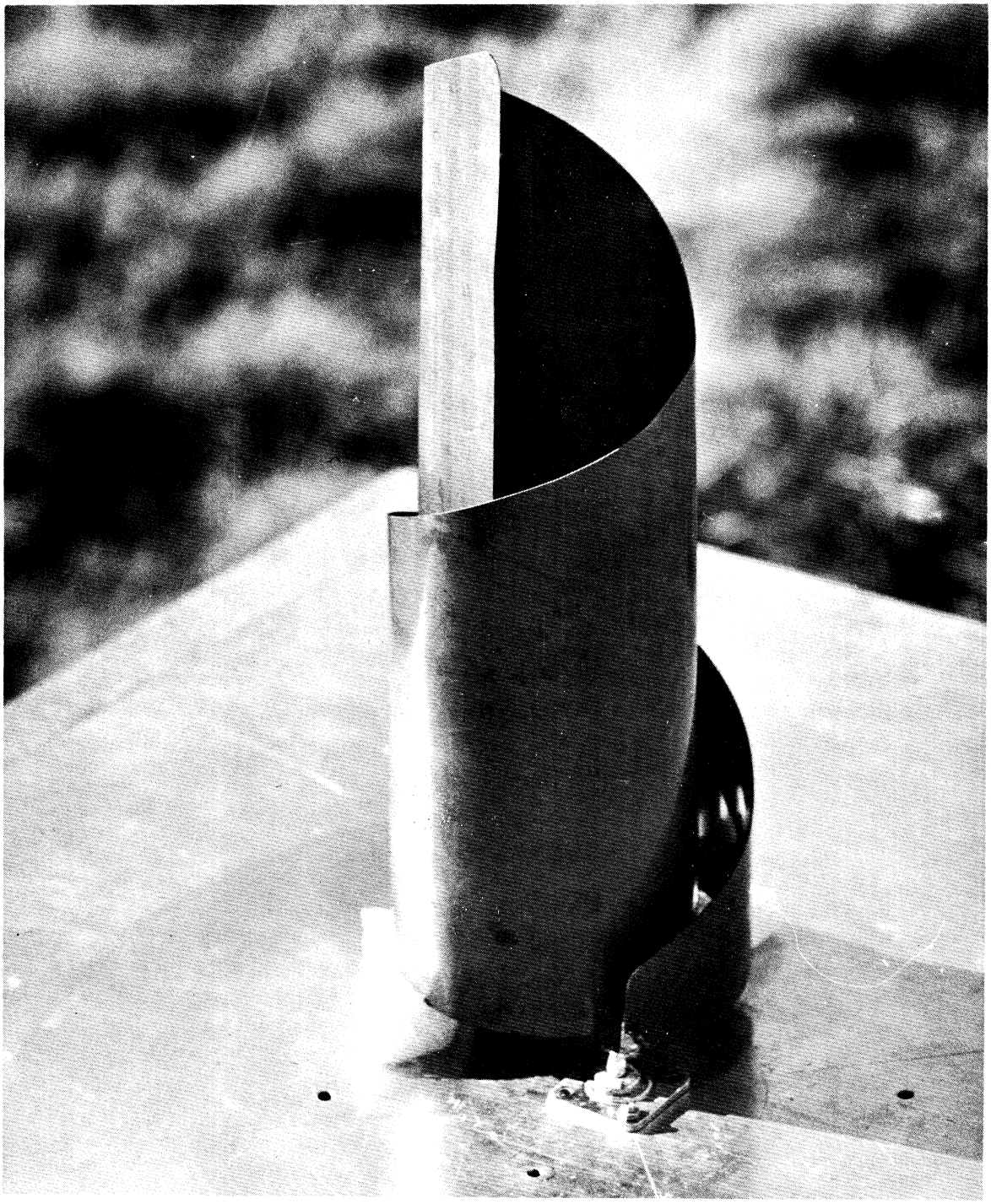

FIG. 12: SPIRALED TRAPEZOID ANTENNA

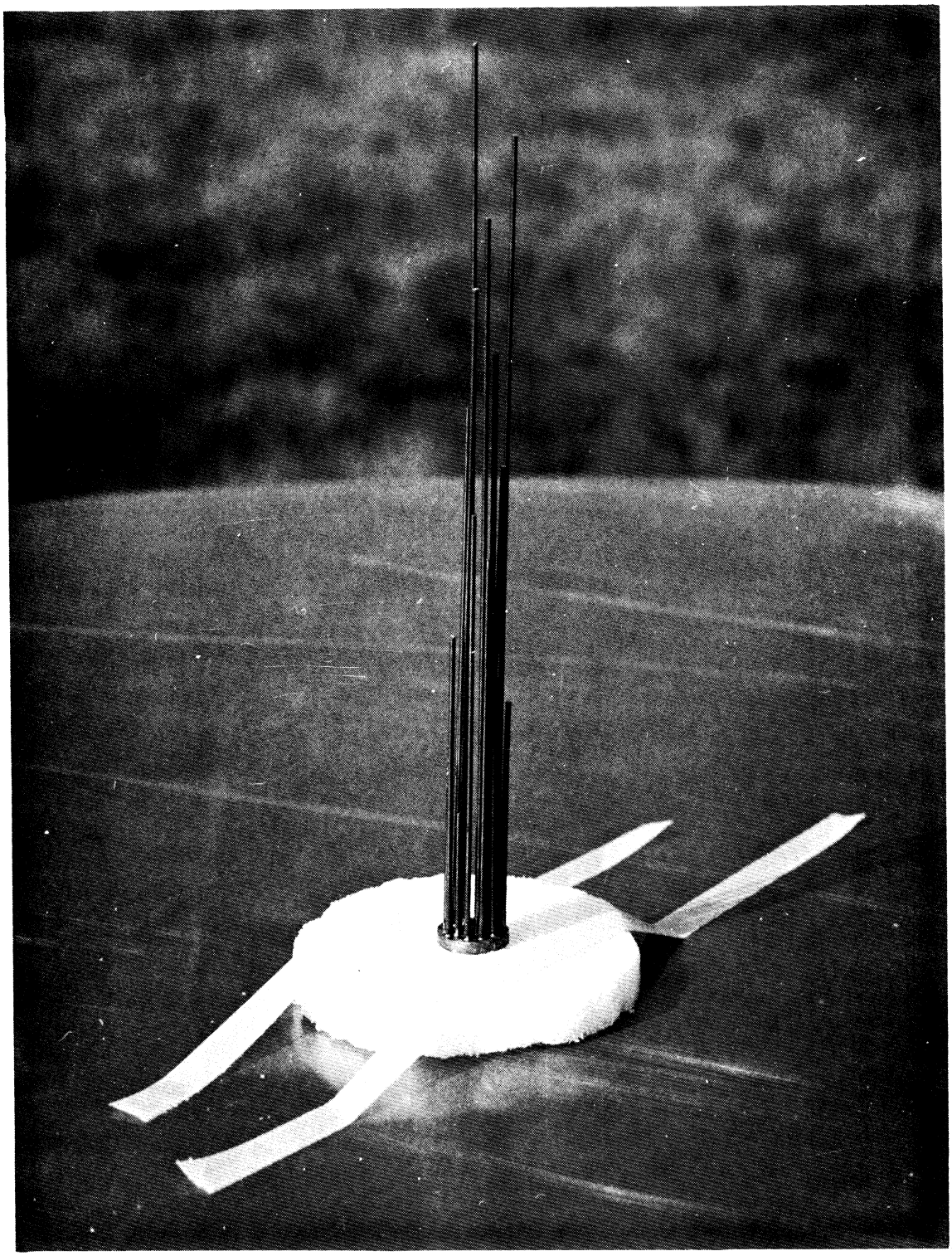

FIG. 13: RANDOM LENGTH ARRAY

Data collected to date has been obtained with the basic element mounted above a large flat ground plane. It is felt that to maintain the broadband characteristics with a small ground plane, it will be necessary to conduct additional tests employing a conical ground plane as noted in 3.1 above.

IV

LOADED CONICAL HELIX ANTENNA

The progress of the loaded conical helix project has been split into two parts; theoretical and experimental. The theoretical part is summarized in the following sections (4.1 — 4.3) where a theoretical solution for full core loading is given (Hong, 1965).

4.1 Propagation Constant

For analysis of a closely wound helix, it is convenient to choose the sheath helix as a mathematical model. The sheath helix is a ficticious model of an actual helix and is pictured in Fig. 14.

The sheath surface is treated as an anisotropic conducting sheath in the sense that current is constrained to flow only in helical paths. The sheath helix supports two sets of modes, TE and TM. The axial electric and magnetic fields of each mode may be represented as:

$$H_z^{i,e} = A_n^{i,e} \begin{cases} I_n(\gamma^i r) \\ K_n(\gamma^e r) \end{cases} e^{-j\beta z - jn\theta} \begin{matrix} r \le a \\ r \ge a \end{matrix} \qquad (19)$$

and

$$E_z^{i,e} = B_n^{i,e} \begin{cases} I_n(\gamma^i r) \\ K_n(\gamma^e r) \end{cases} e^{-j\beta z - jn\theta} \begin{matrix} r \le a \\ r \ge a \end{matrix} \qquad (20)$$

with

$$\gamma^e = \sqrt{\beta^2 - k_o^2}, \qquad \gamma^i = \sqrt{\beta^2 - k_o^2 \epsilon_r \mu r}$$

and

$$k_o = \omega\sqrt{\mu_o \epsilon_o}.$$

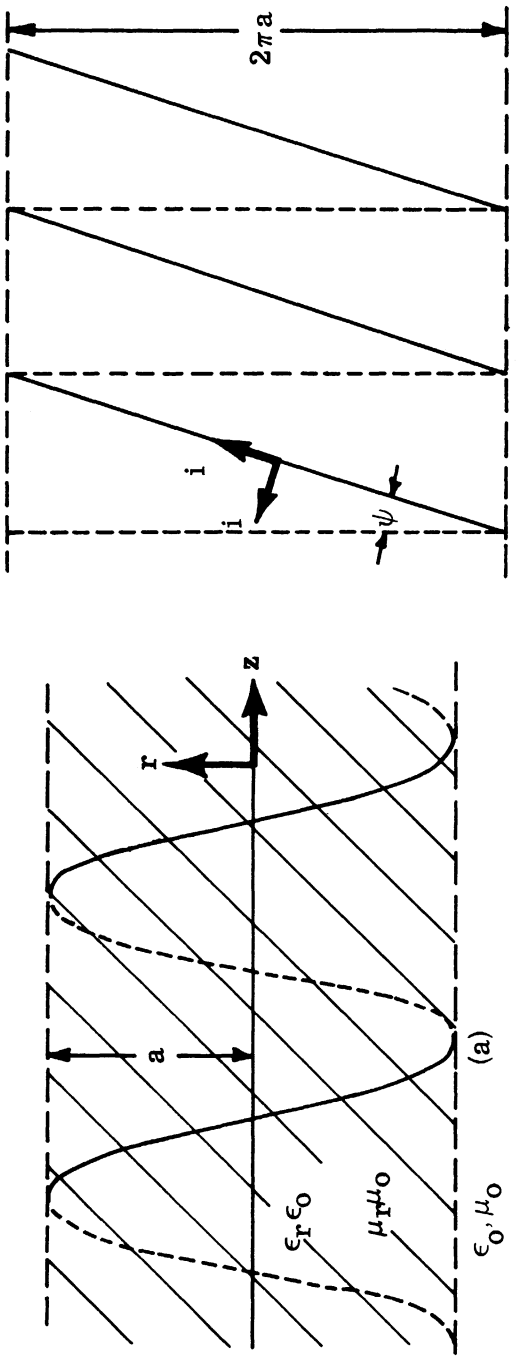

FIG. 14: SHEATH HELIX LOADED WITH MAGNETO-DIELECTRIC MATERIAL
a= radius, ψ = pitching angle, ϵ_r= dielectric constant, μ_r= relative permeability.

I_n and K_n are modified Bessel functions of order n, and the superscripts i and e refer to inside and outside, respectively. The boundary conditions at r = a are: the component of the magnetic field parallel to helical paths is continuous, the component of the electric field normal to helical paths is continuous, and the parallel component of the electric fields are zero. Determining the electric and magnetic fields with Eqs. (19) and (20), and then using these boundary conditions at r = a, one finds that in order to have a non-trivial solution, the following determinantal equation must be satisfied:

$$\frac{K_n(\gamma^e a)}{K_n'(\gamma^e a)} - \frac{k_o^2 a^2 (\gamma^e a)^2 \cot^2\psi}{\left[(\gamma^e a)^2 - n\beta a \cot\psi\right]^2} \cdot \frac{K_n'(\gamma^e a)}{K_n(\gamma^e a)} = A \frac{1}{\mu_r} \frac{I_n(\gamma^i a)}{I_n'(\gamma^i a)} \qquad (21)$$

$$- \frac{k_o^2 a^2 (\gamma^e a)^2 \cot^2\psi}{\left[(\gamma^e a)^2 - n\beta a \cot\psi\right]^2} \cdot \frac{\gamma^e}{\gamma^i} \epsilon_r \frac{I_n'(\gamma^i a)}{I_n(\gamma^i a)}$$

with

$$A = \frac{(\gamma^e)^3}{(\gamma^i)^3} \cdot \left[\frac{(\gamma^i a)^2 - n\beta a \cot\psi}{(\gamma^e a)^2 - n\beta a \cot\psi}\right]^2 . \qquad (22)$$

For slow waves radial propagation constants are almost equal to β, and we can approximate $\gamma^i \simeq \gamma^e = \gamma$. Using this relationship, the approximate solution of Eq. (21) for n = 0 can be easily obtained by the similar method as that used for the unloaded helix (Bevensee, 1964). We obtain the relationship between β and k_o:

$$\frac{k_o a}{\beta a} = \sqrt{\frac{1 + \frac{1}{\mu_r}}{1 + \epsilon_r}} \sin\psi \qquad (23)$$

4.2 Size Reduction for Bifilar Helices

Dyson (1965) has shown that the propagation constant obtained from the sheath model can be applied for analysis of bifilar helix. He has also shown that for a conical helix with a narrow cone angle ($2\theta_o$), analysis of a cylindrical helix can be used with a slight modification. For a conical helix, Eq. (24) is modified as

$$\frac{k_o a}{\beta a} = \sqrt{\frac{1+\frac{1}{\mu_r}}{1+\epsilon_r}} \sin\psi \cos\theta_o . \qquad (24)$$

From Eq. (23), we obtain the Brillouin diagram for a bifilar helix. (see Fig. 15). As frequency changes, the propagation constant β varies along the line:

$$\frac{k_o a}{\beta a} = \sqrt{\frac{1+\frac{1}{\mu_r}}{1+\epsilon_r}} \sin\psi .$$

When this line meets with the line given by $\frac{k_o a}{\cot\psi} = 1 - \frac{\beta a}{\cot\psi}$, the phase of the radiated fields from each element of the helical antenna is lined up such that a backfire radiation occurs (Jones and Mittra, 1965). Figure 15 shows that as the frequency increases further, the radiation pattern changes from backfire to broadside, then to endfire.

The required size of a cylindrical bifilar helix for backfire radiation can be obtained from the solution of the following two equations:

$$\frac{k_o a}{\beta a} = \sqrt{\frac{1+\frac{1}{\mu_r}}{1+\epsilon_r}} \sin\psi \qquad (25)$$

$$\frac{k_o a}{\cot\psi} = 1 - \frac{\beta a}{\cot\psi} .$$

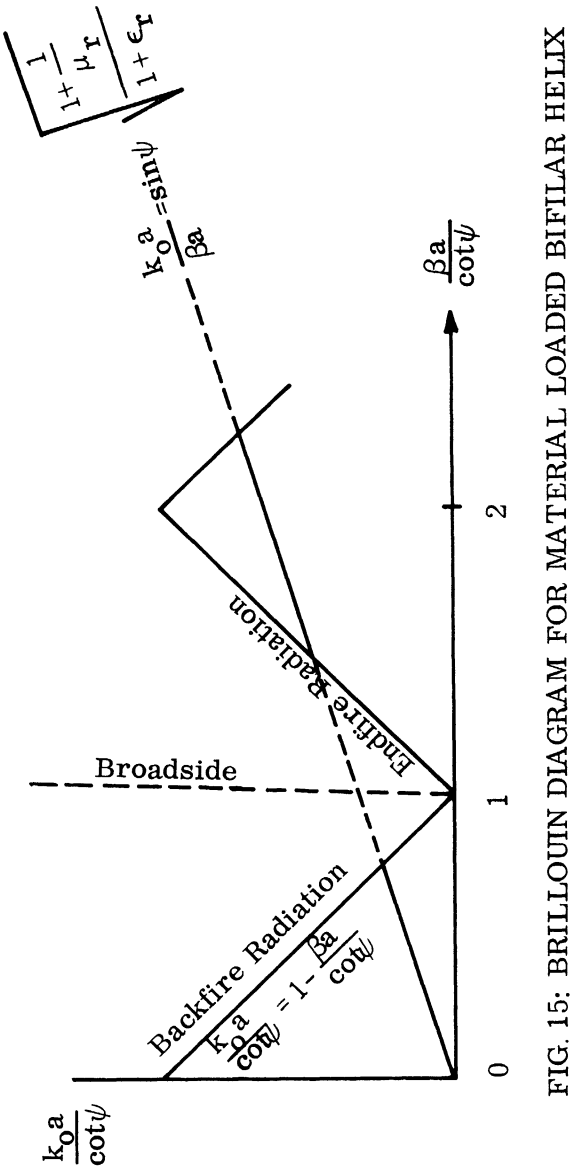

FIG. 15: BRILLOUIN DIAGRAM FOR MATERIAL LOADED BIFILAR HELIX

The solution of Eq. (25) is

$$k_o a = \frac{\sqrt{\dfrac{1+\dfrac{1}{\mu_r}}{1+\epsilon_r}}\cos\psi}{1+\sqrt{\dfrac{1+\dfrac{1}{\mu_r}}{1+\epsilon_r}}\sin\psi} \tag{26}$$

Therefore the ratio between the linear sizes of loaded and unloaded helices becomes

$$\frac{a(\text{with arbitrary } \epsilon_r \text{ and } \mu_r)}{a(\text{with } \epsilon_r = \mu_r = 1)} = \frac{\sqrt{\dfrac{1+\dfrac{1}{\mu_r}}{1+\epsilon_r}}(1+\sin\psi)}{1+\sqrt{\dfrac{1+\dfrac{1}{\mu_r}}{1+\epsilon_r}}\sin\psi} \tag{27}$$

In a similar manner, the active region of a conical bifilar helix for backfire radiation can be predicted from the following formula:

$$k_o a = \frac{\sqrt{\dfrac{1+\dfrac{1}{\mu_r}}{1+\epsilon_r}}\cos\psi \cdot \cos\theta_o}{1+\sqrt{\dfrac{1+\dfrac{1}{\mu_r}}{1+\epsilon_r}}\sin\psi \cdot \cos\theta_o} \tag{28}$$

with $2\theta_o$ = cone angle.

In Eq. (28) 2a is the diameter of the cross section of the cone in the region where helical elements become active and radiates. The linear size reduction factor for a conical helix is

$$\frac{a(\text{arbitrary } \epsilon_r \text{ and } \mu_r)}{a(\epsilon_r = \mu_r = 1)} = \frac{\sqrt{\dfrac{1 + \dfrac{1}{\mu_r}}{1 + \epsilon_r}}\,(1 + \sin\psi \cdot \cos\theta_o)}{1 + \sqrt{\dfrac{1 + \dfrac{1}{\mu_r}}{1 + \epsilon_r}}\,\sin\psi \cdot \cos\theta_o} \tag{29}$$

4.3 Discussion

We have shown in the previous section that the size of the bifilar helical antennas can be reduced by loading the inside of helices with magneto-dielectric material. The linear size reduction factors are given by Eq. (27) for a cylindrical helix, and by Eq. (29) for a conical helix. For example, when a cylindrical bifilar helix with the pitch angle $\psi = 6.5^o$ is loaded with ferrite of $\epsilon_r = 3.77$ and $\mu_r = 2.2$, the ratio of two sizes for loaded and unloaded antennas is 1:1.65. This numerical value agrees with the experimental data obtained by Rassweiler of the Radiation Laboratory (private communication).

Another important conclusion from the present analysis is the following: when the size reduction factor is specified, we can choose any materials with arbitrary combination of ϵ_r and μ_r, as long as

$$\sqrt{1 + \frac{1}{\mu_r}} \Big/ \sqrt{1 + \epsilon_r}$$

remains constant. This is a very useful aspect. As it is well known, electric properties of magneto-dielectric material changes as frequency varies in wide range. For example, different materials have different frequency ranges where energy loss due to material loaded inside of helices is minimum. When the weight of the antenna loaded with certain material is too heavy for mobile or airborne use, it may be replaced by another material whose weight per volume is less, but whose reduction factor remains unchanged.

Extension to a monofilar antenna loaded with magneto-dielectric is simple. We can obtain the reduction factor by merely modifying the Brillouin diagram of Fig. 15.

The question to be solved in the future is: Do we have to load the inside of a helix completely, or is partial loading enough to keep the desired radiation pattern and the size reduction factor? It is desirable to find out the minimum thickness of the magneto-dielectric load in order to improve efficiency and to reduce the weight of the antenna.

4.4 Experimental Results

The experimental portion of this project has concentrated on the measurement of patterns of loaded and unloaded bifilar helices in order to verify full-core loading theory, and to investigate the effect of an interior layer loading fitted flush to the helix windings. Previous investigations have demonstrated size reduction (Lyon et al, 1965). Table II shows the results so far of many pattern measurements.

Figures 16 - 19 give typical patterns for the bifilar helices tested with various loadings. To assemble the loaded bifilar helix, a stripped coaxial cable which serviced as the helix conductor was wound on a thin fiberglas form. The loading powder was poured inside. Layers of the loading material were achieved by using a balsa wood core to approximate an air core. Far field patterns were then taken to ascertain loading. Since helical antennas are wide band, the determination of a precise center frequency is difficult. Experimental near-field phase measurements are planned.

The experimental results indicate:

1) Good agreement with theory in some cases is obtained. More data is needed for complete verification.

2) A rather thin material layer reduces the helix size, although to a slightly less extent than obtained with a full core.

3) A supplementary method of experimental evaluation in addition to far-field measurements would be helpful in further assessment of theoretical results. With this in mind, near field measurements are planned.

4.5 Discussion of Possible Prototype

The results of investigations of magneto-dielectric loading of helices indicate that one promising loading would consist of layered dielectric inside the cone holding the conductor. The present concept is to have a collapsible log-spiral antenna of pyramidal form similar to previously designed collapsible umbrella-like structures (Fig. 20). The dielectric loading slabs would be stored separately and placed

inside the antenna windings after setting up the antenna. In order to maintain light weight, an artificial dielectric foam is being investigated (Emerson and Cuming, Eccofoam, High-K Flexible, $\epsilon \geq 6$).

TABLE II: Results of Pattern Measurements

Material ϵ	Material μ	Loading	Radius Reduction Factor Experiment ($\pm$ 10 percent)	Theory*
3.8	2.2	Full core	.63	.60
3.8	2.2	.04, .02, .01λ	.63	-
10.	1.	.01λ	.55 ($\pm$ 15 percent)	.45
3.8	2.2	.006λ	.77	.60
10.	1.	.006λ	.77	.45

* Theory applies to full core only with materials as listed.

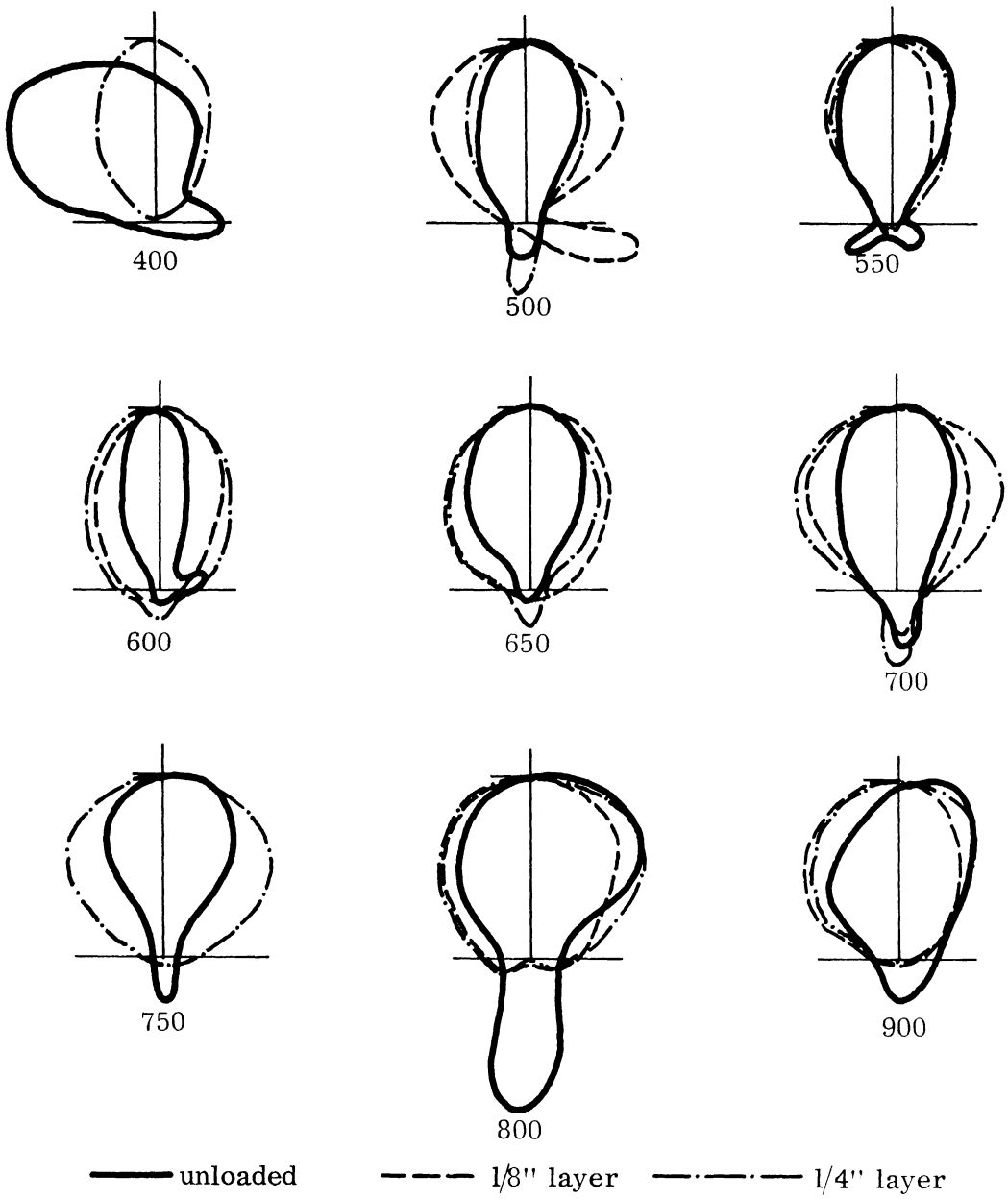

FIG. 16: HELIX WITH DIELECTRIC LOADING Plots of E_{ϕ}^{2}. Dielectric ϵ=10. Helix Diameter = 4.5".

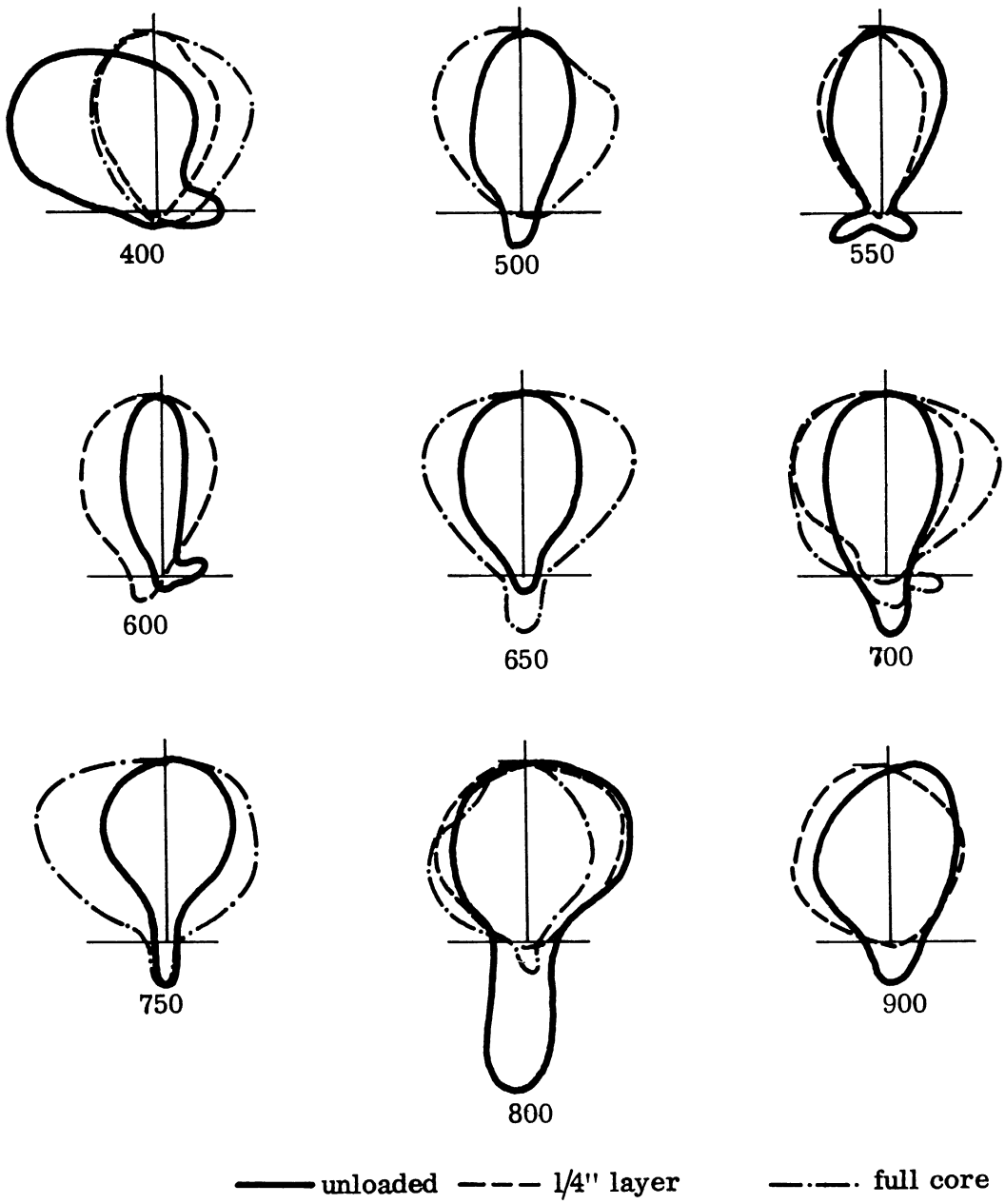

FIG. 17: HELIX WITH THICK LAYER FERRITE LOADING
Linear plots of E_ϕ^2. Ferrite μ=2.2, ϵ=3.8, Helix Diameter = 4.5".

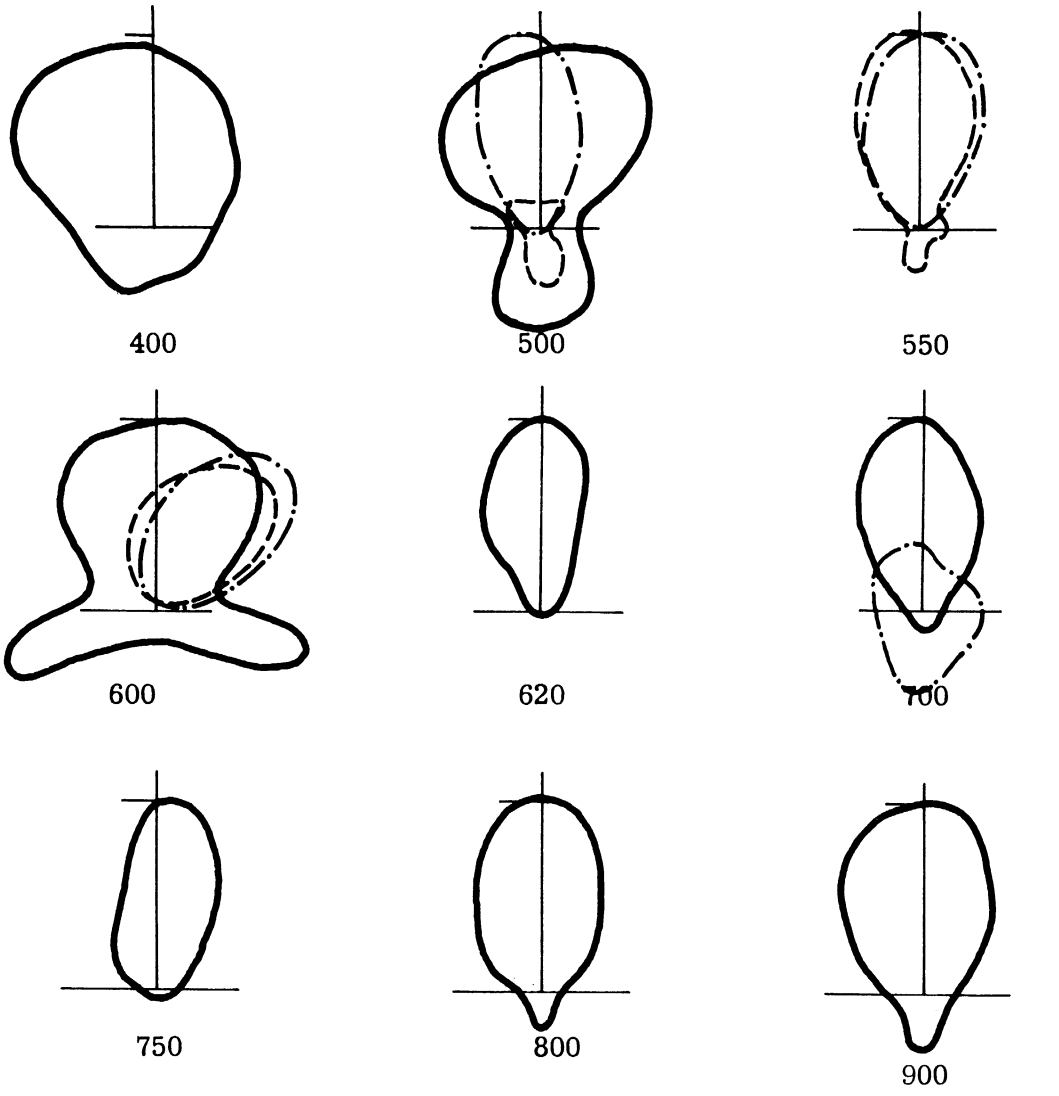

FIG 18: HELIX WITH THICK LAYER FERRITE LOADING
Plot of E_{ϕ}^{2}, Ferrite μ =2.2, ϵ = 3.8, Helix Diameter = 4" .

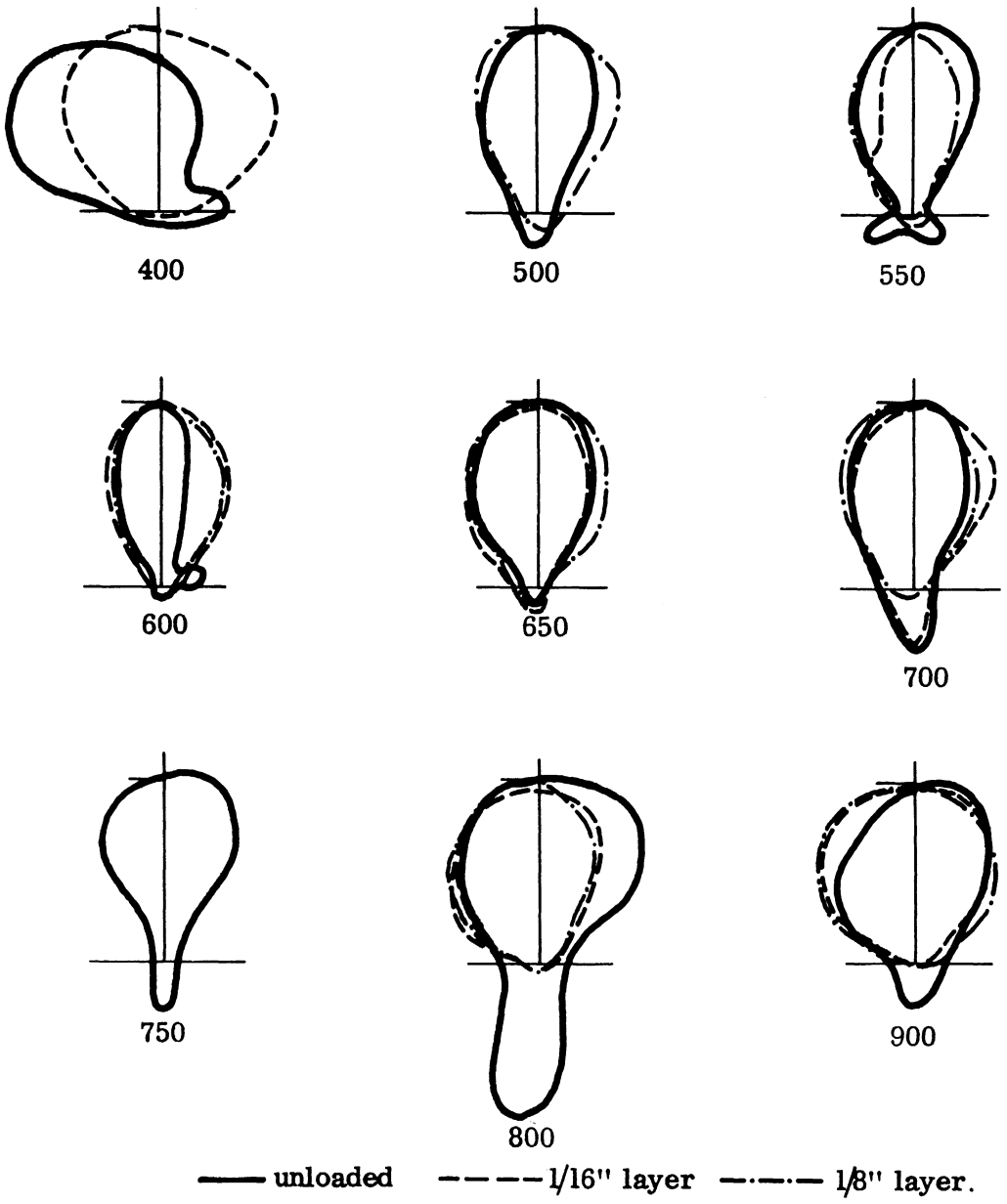

FIG 19: HELIX WITH THIN LAYER FERRITE LOADING
Linear plots of E_ϕ^2, Ferrite μ = 2.2, ϵ = 3.8, Helix Diameter = 4.5"

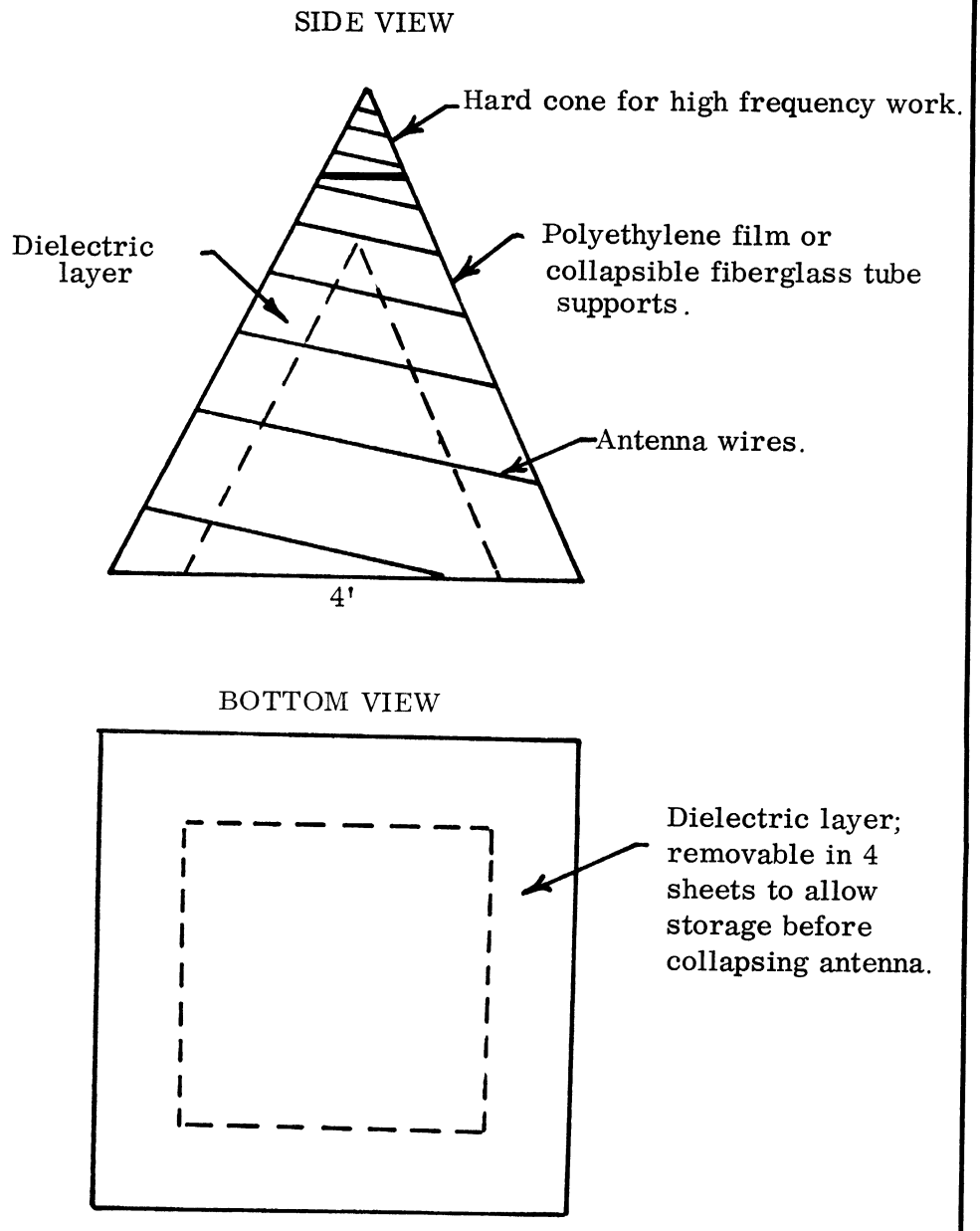

FIG. 20: PROPOSED PROTOTYPE FOR LOADED CONICAL LOG-SPIRAL ANTENNA

V
REFERENCES

Bevensee, R.M. (1964), Electromagnetic Slow Wave Systems, J. Wiley and Sons Inc., New York

Brown, G.H. and O.M. Woodward, Jr. (1952), "Experimentally Determined Radiation Characteristics of Conical and Triangular Antennas," RCA Reviews pp. 425-450.

Dorne, A. and O. Lazarus (1947), Very High Frequency Techniques, McGraw-Hill, New York, pp. 174-176.

Duncan, J.W. and V.P. Minerva (1960), "100:1 Bandwidth Balun Transformer," Proc. IRE, 48, pp. 156-164.

Dyson, J.D. (1965), "The Characteristics and Design of the Conical Log-Spiral Antenna, " IEEE Trans. G-AP, AP-13, pp. 488-499.

Ferris, J.E. et al (1965), "Broadband Antenna Techniques Study," First Quarterly Report ECOM 01263-1, USAEC Contract DA 28-043 AMC-01263(E), Radiation Laboratory Report 07260-1-Q.

Gans, M., D. Kayfez and V.H. Rumsey (1965), "Frequency Independent Baluns", Proc. IRE, 53, pp. 647-648.

Hong, S. (1965), "Size Reduction of Bifilar Helical Antennas by Loading with Magneto-Dielectric Material, " Radiation Laboratory Internal Memorandum No. 07260-504-M.

Jasik, H. (1961), Antenna Engineering Handbook, McGraw-Hill, New York, pp. 3-24.

Jones, K.E. and Mittra, R. (1965), "Some Interpretations and Applications of the K-β Diagram", University of Illinois Antenna Laboratory Report 65-1.

King, R.W. (1956), The Theory of Linear Antennas, Harvard University Press, pp. 808-815.

Lamberty, B.J. (1958), "A Class of Low Gain Broadband Antennas", IRE WESCON Convention Record, Pt. 1, pp. 251-259.

Lyon, J.A.M., et al (1965), "Study and Investigation of a UHF-VHF Antenna - Final Report, "AFAL-TR-65-4, University of Michigan Radiation Laboratory Report 5549-1-F.

Mumford, W.W. (1961), "Some Technical Aspects of Microwave Radiation Hazards", Proc. IRE, 49, pp. 427-447.

Schelkunoff, S.A. (1943), Electromagnetic Waves, D Van Nostrand Co., New York

DISTRIBUTION LIST

Address	Copies
Defense Documentation Center Attn: TISIA Cameron Station (Bldg. 5) Alexandria, Virginia 22314	20
Office of Assistant Secretary of Defense (Research and Development) Attn: Technical Library, Rm. 3E1065 Washington, D. C. 20315	1
Director, U S Naval Research Laboratory Attn: Code 2027 Washington, D. C. 20390	1
CO and Director, U S Navy Electronics Laboratory Attn: Library San Diego, California 92101	1
AFSC Scientific / Technical Liaison Office U S Naval Air Development Center Johnsville, Pennsylvania 18974	1
Systems Engineering Group (SEPIR) Wright-Patterson AFB, Ohio 45433	1
Electronic Systems Division (AFSC) Scientific / Technical Information Division ESTI L. G. Hanscom Field Bedford, Massachusetts 01731	1
Air Force Cambridge Research Laboratories Attn: CRXL-R L. G. Hanscom Field Bedford, Massachusetts 01731	1
Chief of Research and Development Department of the Army Washington, D. C. 20315	1
C.G., U. S. Army Material Command Attn: R and D Directorate Washington, D. C. 20315	2

Commanding General
U. S. Army Electronic Command
Attn: AMSEL-KL-EM
Fort Monmouth, New Jersey 07703 1

C. G., U.S. Army Combat Development Command
Communications - Electronics Agency
Fort Huachuca, Arizona 85613 1

Commanding General
U. S. Army Security Agency
Attn: IADEV
Arlington Hall Station
Arlington, Va. 22207 3

C.O., Harry Diamond Laboratories
Connecticut Ave and Van Ness St., N.W.
Washington, D.C. 20438 1

C.G., U. S. Army Electronic Proving Ground
Attn: Technical Library
Fort Huachuca, Arizona 85613 1

C.G., U. S. Army Electronics Command
Attn: AMSEL-WL-S
Fort Monmouth, New Jersey 07703 3

C. G., U. S. Army Electronics Command
Attn: AMSEL-RD-DR
Fort Monmouth, New Jersey 07703 1

C. G., U. S. Army Electronics Command
Attn: AMSEL-RD-ADT
Fort Monmouth, New Jersey 07703 1

C. G., U. S. Army Electronics Command
Attn: AMSEL-RD-ADO-RHA
Fort Monmouth, New Jersey 07703 1

C. G., U. S. Army Electronics Command
Attn: AMSEL-RD-LNA
Fort Monmouth, New Jersey 07703 1

C. G., U. S. Army Electronics Command
Attn: AMSEL-RD-LNR
Fort Monmouth, New Jersey 07703 — 1

Dir., Material Readiness Directorate, AMSEL-MR
U. S. Army Electronics Command
Fort Monmouth, New Jersey 07703

C. O., U. S. Army Electronics R and D Activity
Attn: SELWS-AJ
White Sands, New Mexico 88002 — 1

Chief, U. S. Army Electronics Laboratories
Mountain View Office
P. O. Box 205
Mountain View, California 94042 — 1

U. S. Army Electronics Laboratories Liaison Officer
Rome Air Development Center
Attn: RAOL
Griffiss AFB, New York 13442 — 1

U. S. National Bureau of Standards
Boulder Laboratories
Attn: Library
Boulder, Colorado — 1

Total — 49

DOCUMENT CONTROL DATA - R&D

(Security classification of title, body of abstract and indexing annotation must be entered when the overall report is classified)

1. ORIGINATING ACTIVITY (Corporate author) The University of Michigan Radiation Laboratory Department of Electrical Engineering Ann Arbor, Michigan 48108	2a. REPORT SECURITY CLASSIFICATION UNCLASSIFIED 2b. GROUP

3. REPORT TITLE

BROADBAND ANTENNA TECHNIQUES STUDY

4. DESCRIPTIVE NOTES (Type of report and inclusive dates)

Second Quarterly Report, 1 July - 30 September 1965

5. AUTHOR(S) (Last name, first name, initial)

Ferris, Joseph E., Hong, Soonsung, Lyon, John A. M., Rassweiler, George G. and Zimmerman, Wiley E.

6. REPORT DATE	7a. TOTAL NO. OF PAGES	7b. NO. OF REFS
November 1965	48	15

8a. CONTRACT OR GRANT NO. DA 28-043-AMC-01263(E) b. PROJECT NO. 5A0-21101-A902-01-08 c. d.	9a. ORIGINATOR'S REPORT NUMBER(S) 7260-2-Q 9b. OTHER REPORT NO(S) (Any other numbers that may be assigned this report) ECOM 01263-2

10. AVAILABILITY/LIMITATION NOTICES

Each transmittal of this document outside the Department of Defense must have prior approval of the United States Electronics Command, AMSEL-WL-S, Ft. Monmouth, N. J.

11. SUPPLEMENTARY NOTES	12. SPONSORING MILITARY ACTIVITY
	United States Army Electronics Command Fort Monmouth, New Jersey 07703

13. ABSTRACT

Work on the design, fabrication and testing of three broadband antennas is described. The antenna types are, 1) high-gain constant beamwidth, 2) omnidirectional and 3) loaded conical helix.

During this period the optimum F/D ratio for the reflector of the high gain constant beamwidth antenna has been determined. A decision has also been made to have the reflector surface fabricated from fiberglas and, therefore, a plaster mold has been constructed. In the proposal, several techniaues were suggested by which the constant beamwidth characteristics of the antenna could be achieved. During this reporting period the feasibility of using a wire grid structure as a reflecting surface has been considered and is reported.

Four antenna types have been considered to meet the omnidirectional antenna requirements. The types considered are, biconical, crossed plate, spiraled trapezoid and a random length array. A thorough discussion of the biconical antenna is included which demonstrates both its advantages and sisadvantages. Also a discussion of dipole vs monopole configurations is included to aid in the understanding of the problem associated with broadband omni-directional antennas.

A theoretical solution for the size reduction of a helix antenna loaded with a full core of magneto-dielectric material is discussed. The reduction formula indicates the permittivity to be more important than the permeability of the loading material. Experimental far-field patterns of the loaded helix antenna are shown which partially support the analysis.

DD FORM 1 JAN 64 1473

14. KEY WORDS	LINK A		LINK B		LINK C	
	ROLE	WT	ROLE	WT	ROLE	WT
BROADBAND CONSTANT BEAMWIDTH OMNIDIRECTIONAL SIZE REDUCTION ANTENNA BEAM SHAPING RIDGED HORN CROSSED PLATE ANTENNA LOADED HELIX LOADED CONICAL HELIX						

INSTRUCTIONS

1. ORIGINATING ACTIVITY: Enter the name and address of the contractor, subcontractor, grantee, Department of Defense activity or other organization *(corporate author)* issuing the report.

2*a*. REPORT SECURITY CLASSIFICATION: Enter the overall security classification of the report. Indicate whether "Restricted Data" is included. Marking is to be in accordance with appropriate security regulations.

2*b*. GROUP: Automatic downgrading is specified in DoD Directive 5200.10 and Armed Forces Industrial Manual. Enter the group number. Also, when applicable, show that optional markings have been used for Group 3 and Group 4 as authorized.

3. REPORT TITLE: Enter the complete report title in all capital letters. Titles in all cases should be unclassified. If a meaningful title cannot be selected without classification, show title classification in all capitals in parenthesis immediately following the title.

4. DESCRIPTIVE NOTES: If appropriate, enter the type of report, e.g., interim, progress, summary, annual, or final. Give the inclusive dates when a specific reporting period is covered.

5. AUTHOR(S): Enter the name(s) of author(s) as shown on or in the report. Enter last name, first name, middle initial. If military, show rank and branch of service. The name of the principal author is an absolute minimum requirement.

6. REPORT DATE: Enter the date of the report as day, month, year; or month, year. If more than one date appears on the report, use date of publication.

7*a*. TOTAL NUMBER OF PAGES: The total page count should follow normal pagination procedures, i.e., enter the number of pages containing information.

7*b*. NUMBER OF REFERENCES: Enter the total number of references cited in the report.

8*a*. CONTRACT OR GRANT NUMBER: If appropriate, enter the applicable number of the contract or grant under which the report was written.

8*b*, 8*c*, & 8*d*. PROJECT NUMBER: Enter the appropriate military department identification, such as project number, subproject number, system numbers, task number, etc.

9*a*. ORIGINATOR'S REPORT NUMBER(S): Enter the official report number by which the document will be identified and controlled by the originating activity. This number must be unique to this report.

9*b*. OTHER REPORT NUMBER(S): If the report has been assigned any other report numbers *(either by the originator or by the sponsor)*, also enter this number(s).

10. AVAILABILITY/LIMITATION NOTICES: Enter any limitations on further dissemination of the report, other than those imposed by security classification, using standard statements such as:

(1) "Qualified requesters may obtain copies of this report from DDC."

(2) "Foreign announcement and dissemination of this report by DDC is not authorized."

(3) "U. S. Government agencies may obtain copies of this report directly from DDC. Other qualified DDC users shall request through

_____."

(4) "U. S. military agencies may obtain copies of this report directly from DDC. Other qualified users shall request through

_____."

(5) "All distribution of this report is controlled. Qualified DDC users shall request through

_____."

If the report has been furnished to the Office of Technical Services, Department of Commerce, for sale to the public, indicate this fact and enter the price, if known.

11. SUPPLEMENTARY NOTES: Use for additional explanatory notes.

12. SPONSORING MILITARY ACTIVITY: Enter the name of the departmental project office or laboratory sponsoring *(paying for)* the research and development. Include address.

13. ABSTRACT: Enter an abstract giving a brief and factual summary of the document indicative of the report, even though it may also appear elsewhere in the body of the technical report. If additional space is required, a continuation sheet shall be attached.

It is highly desirable that the abstract of classified reports be unclassified. Each paragraph of the abstract shall end with an indication of the military security classification of the information in the paragraph, represented as *(TS), (S), (C), or (U)*.

There is no limitation on the length of the abstract. However, the suggested length is from 150 to 225 words.

14. KEY WORDS: Key words are technically meaningful terms or short phrases that characterize a report and may be used as index entries for cataloging the report. Key words must be selected so that no security classification is required. Identifiers, such as equipment model designation, trade name, military project code name, geographic location, may be used as key words but will be followed by an indication of technical context. The assignment of links, rules, and weights is optional.